cosmetics

MDPI

Article

FTIR- and LC-MS/MS-Identified Phytochemicals and In Vitro Cytotoxic, Antioxidant and Anti-Inflammatory Activities of *Oroxylum indicum* Extracts Obtained by Microwave-Assisted Extraction

Panisara Rachprasit [1], Santi Phosri [2], Sukanya Tastub [3], Sarita Sangthong [1,4], Phanuphong Chaiwut [1,4], Lutfun Nahar [5], Satyajit D. Sarker [6] and Tinnakorn Theansungnoen [1,*]

[1] School of Cosmetic Science, Mae Fah Luang University, Chiang Rai 57100, Thailand; 6671704003@lamduan.mfu.ac.th (P.R.); sarita.san@mfu.ac.th (S.S.); phanuphong@mfu.ac.th (P.C.)
[2] Department of Chemical Engineering, Faculty of Engineering, Burapha University, Chonburi 20131, Thailand; santi.ph@eng.buu.ac.th
[3] Synchrotron Light Research Institute (Public Organization), Nakhon Ratchasima 30000, Thailand; sukanya@slri.or.th
[4] Green Cosmetic Technology Research Group, School of Cosmetic Science, Mae Fah Luang University, Chiang Rai 57100, Thailand
[5] Laboratory of Growth Regulators, Institute of Experimental Botany, Palacký University, The Czech Academy of Sciences, Šlechtitelů 27, CZ-783 71 Olomouc, Czech Republic; profnahar@outlook.com
[6] Centre for Natural Products Discovery, School of Pharmacy and Biomolecular Sciences, Liverpool John Moores University, Byrom Street, Liverpool L3 3AF, UK; s.sarker@ljmu.ac.uk
* Correspondence: tinnakorn.the@mfu.ac.th

Abstract

Acne vulgaris is a chronic inflammatory disorder of the pilosebaceous units. Although the overcolonization of *Cutibacterium acnes* is a primary contributor to acne development, acne-related inflammation is typically driven by a combination of pro-inflammatory cytokines and oxidative stress mediated by reactive oxygen species (ROS). This study aimed to screen extracts of *Oroxylum indicum* to assess its potential as an anti-acne candidate for cosmetic formulations. Bark (OB), leaf (OL), pod (OP), and seed (OS) extracts of *O. indicum* were obtained by microwave-assisted extraction (MAE) with 50% (*v*/*v*) and 70% (*v*/*v*) aqueous ethanol. The extracts were subjected to UV–Vis and Fourier transform infrared (FTIR) spectroscopic analyses and skin-related cytotoxicity, antioxidant, and anti-inflammatory activity assays. UV–Vis and FTIR spectral analyses suggested the presence of phenolic compounds in *O. indicum* extracts. The antioxidant (free-radical-scavenging) activity of most extracts against DPPH radicals was evident from their IC_{50} values ranging between 0.35 ± 0.06 mg/mL and 0.54 ± 0.04 mg/mL, while that of MAE-OB50 and MAE-OP50 was 1.04 ± 0.08 mg/mL and 1.06 ± 0.15 mg/mL, respectively. Most extracts, with the exception of the pod extracts, exhibited a low level of cytotoxicity at 200 µg/mL in HaCaT and MRC-5 cells. Anti-inflammatory activities affecting nitric oxide (NO) production were observed in the *O. indicum* extracts MAE-OL50 (IC_{50}: 128.00 ± 2.80 µg/mL), MAE-OB70 (IC_{50}: 178.72 ± 3.52 µg/mL), MAE-OL70 (IC_{50}: 126.26 ± 0.71 µg/mL), and MAE-OS70 (IC_{50}: 147.03 ± 0.59 µg/mL). The predominant phytochemicals in MAE-OL50, MAE-OB70, MAE-OL70, and MAE-OS70, tentatively identified by liquid chromatography–tandem mass spectrometry (LC-MS/MS), belong to flavonoids and their glycosides, methoxylated flavones, isoflavones, phenolic glycosides, and sugar-related metabolites. The results suggest that *O. indicum* extracts could be promising candidate ingredients for cosmetic formulations

Academic Editor: Enzo Berardesca

Received: 29 September 2026
Revised: 8 November 2026
Accepted: 8 November 2026
Published: 11 November 2026

Copyright: © 2026 by the authors. Licensee MDPI, Basel, Switzerland. This article is an open access article distributed under the terms and conditions of the Creative Commons Attribution (CC BY) license.

targeting inflammation-associated and oxidative stress-related skin concerns, such as acne-prone skin.

Keywords: *Oroxylum indicum*; anti-inflammatory activity; cytotoxicity; FTIR; LC-MS/MS; microwave-assisted extraction

1. Introduction

Acne vulgaris is a common chronic inflammatory disorder of the pilosebaceous units, affecting approximately 9.4% of the global population and ranking as the eighth most prevalent skin disease, with a particularly high prevalence among adolescents (>85%) [1,2]. It typically manifests in sebaceous gland-rich areas such as the face, chest, and back, presenting as non-inflammatory (comedones) and inflammatory (papules, pustules) lesions that may lead to scarring and a negative impact on psychological well-being [3,4]. The pathogenesis of acne involves follicular hyperkeratinization, increased sebum production, overcolonization of *Cutibacterium acnes*, and inflammation, with inflammation and immune responses recognized as the main pathological features throughout the progression of the disorder [5,6].

Inflammation in acne can be triggered by multiple factors, primarily overcolonization of *C. acnes* along with other bacteria, including Gram-positive strains and Gram-negative strains [7,8]. Bacterial components such as lipopolysaccharide (LPS) activate macrophages, a key component of the innate immune system, triggering the release of pro-inflammatory mediators [9,10]. This is followed by neutrophil recruitment and the generation of reactive oxygen species (ROS), contributing to oxidative stress and tissue damage at inflammation sites [11–13]. Therefore, acne-related inflammation is driven by a combination of pro-inflammatory mediators and ROS-induced oxidative stress, providing the rationale for evaluating both antioxidant and anti-inflammatory activities as an initial screening approach for candidate cosmetic ingredients.

Oroxylum indicum (L.) Benth. ex Kurz, a deciduous tree belonging to the Bignoniaceae family, is a culturally significant plant widely used in Asia, particularly China, Japan, and Thailand, not only as a food source but also as a traditional remedy. The fruit pod is rich in nutrients, including dietary fiber, essential amino acids, and fatty acids [14]. The seed has been used to relieve coughs and bronchitis [15,16]. The bark has been employed to alleviate diarrhea and gastrointestinal discomfort, while the leaf and seed are commonly consumed as herbal preparations or beverages [17]. Consistent with these traditional uses, pharmacological studies have reported *O. indicum* to possess antioxidant, anti-inflammatory, antimicrobial, and immunostimulant activities [18–20]. Previous studies have demonstrated that various extraction approaches applied to the aerial parts of *O. indicum* yield extracts with significant biological activities, particularly when ethanol-based methods such as maceration and Soxhlet extraction are employed, producing extracts rich in flavonoids [21,22].

The effectiveness of plant-based research is strongly influenced by the extraction technique employed. Conventional methods, such as Soxhlet extraction and maceration, are typically associated with prolonged processing times, high solvent consumption, and the risk of thermal degradation in heat-sensitive bioactive compounds. Microwave-assisted extraction (MAE) has emerged as an advanced and environmentally friendly alternative, utilizing microwave energy to rapidly heat plant matrices internally. This process enhances cell wall disruption and facilitates the efficient release of target compounds into the extraction solvent. MAE offers several key advantages, including reduced extraction time, lower solvent usage, increased extraction efficiency, and improved preservation of

bioactive constituents, making it a highly effective approach for the recovery of phytochemicals from plant materials [23].

Therefore, this study provides a comparative evaluation of aqueous ethanolic extracts from the bark, leaves, pods, and seeds of *O. indicum*, obtained under identical MAE conditions, for cosmetic applications. The extracts were evaluated for their antioxidant, anti-inflammatory (NO inhibition), and in vitro cytotoxic activities to explore their preliminary potential as candidate active ingredients for cosmetic formulations targeting inflammation-associated skin concerns. In addition, the phytochemical profiles of the extracts were analyzed using Fourier Transform Infrared (FTIR) spectroscopy and liquid chromatography–tandem mass spectrometry (LC-MS/MS) for tentative compound identification.

2. Materials and Methods

2.1. Chemicals and Reagents

Ethanol (EtOH), methanol (MeOH), and dimethyl sulfoxide (DMSO) were purchased from LabScan Asia Co. (Bangkok, Thailand). 2,2-diphenyl-1-picrylhydrazyl (DPPH) was obtained from Sigma-Aldrich (St. Louis, MO, USA). These solvents and reagents were used for the extraction and analytical processing of the *O. indicum* extracts. L-(+)-ascorbic acid (CAS No. 50-81-7) from Univar/Ajax Finechem (Sydney, Australia) was used as a standard in the analytical process. Dulbecco's modified Eagle's medium (DMEM) complete medium containing 10% fetal bovine serum, 1% L-glutamine, and 1% penicillin/streptomycin was obtained from Gibco (Grand Island, NY, USA). Lipopolysaccharide (LPS) was purchased from Sigma-Aldrich (Taufkirchen, Germany). 3-[4,5-dimethylthiazol-2-yl]-2,5 diphenyl tetrazolium bromide (MTT), acetonitrile and deionized water were purchased from VWR international limited (Lutterworth, UK). All chemicals and reagents used were of analytical reagent (AR) grade.

2.2. Materials and Their Preparation

Four aerial parts of *O. indicum* (L.) Benth. ex Kurz, including bark, leaf, pod, and seed, were purchased as commercially available raw material from a local farmer in Chonburi, Thailand. One kilogram of each plant part was washed, cut into small pieces, and dried separately using a hot air oven at 50 °C. The dried plants were ground into powder using a cutting mill/grinder (SM300, RETSCH GmbH, Haan, Germany) with a 0.5 mm sieve.

2.3. Microwave-Assisted Extraction

Microwave-assisted extraction of the bark, leaf, pod, and seed of *O. indicum* was performed following a modified method of Gunalan et al. (2023) [24]. Each plant powder sample was taken for extraction using aqueous ethanol at varying concentrations (50% and 70%) with an ETHOS™ X microwave extraction system. The sample-to-solvent ratio was 1:30 (*w*/*v*). The extraction was performed under continuous stirring at 600 W and 65 °C for 30 min for two consecutive cycles, with fresh solvent added in each cycle to enhance extraction efficiency. The resulting extracts were filtered through Whatman® No. 1 filter paper (Whatman International Ltd., Maidstone, UK). The filtrates were pooled and subsequently concentrated using a rotary evaporator at 50 °C and 75 mbar. The crude extracts were then stored at 4 °C until further analysis. The extraction yield (%) was calculated using the following equation:

$$\% \text{ Yield} = [(\text{Weight of dry extract})/(\text{Weight of dry plant})] \times 100$$

2.4. UV–Vis Spectrophotometric Analysis

O. indicum extracts were subjected to UV–Vis scanning analysis. The extracts were dissolved in their extraction solvents to prepare a stock 10 mg/mL, which was diluted 10-fold twice (100-fold overall) in the same solvent at room temperature to give a final concentration of 100 μg/mL for all extracts. The absorbance spectra were recorded over a wavelength range of 200–800 nm using a UV–Vis spectrophotometer (UV-Libra S80, Biochrom Ltd., Cambridge, UK) with 10 mm path length quartz cuvettes, and the corresponding extraction solvent was used as the blank.

2.5. FTIR Spectroscopic Analysis

O. indicum extracts were analyzed for functional groups using attenuated total reflectance–Fourier transform infrared (ATR-FTIR) spectroscopy. A Bruker Tensor 27 FTIR spectrometer was used, equipped with a DTGS detector and a single-reflection diamond ATR accessory [Platinum ATR, Bruker Optics]. A 2 μL aliquot of each extract sample was deposited onto the diamond crystal maintained at 45 °C and allowed to dry before measurement. A background spectrum of the clean, dry crystal was recorded before each sample measurement. Each spectrum was acquired with 64 scans at a spectral resolution of 4 cm^{-1}. The spectra were recorded over the range of 4000–650 cm^{-1}. Between measurements, the crystal was cleaned with ethanol and dried. The spectral data were processed using Optical User Software (OPUS) version 7.5 (Bruker Optics Ltd., Ettlingen, Germany).

2.6. Principal Component Analysis

The FTIR spectra of *O. indicum* extracts were further analyzed using principal component analysis (PCA). PCA is particularly effective for interpreting FTIR spectra, which often exhibit substantial band diversity and complexity depending on the sample source [25]. For each extract, FTIR measurements were performed in 100 replicates. The collected spectral dataset was then processed using PCA to distinguish between sample groups, employing Unscrambler X version 10.1 (Camo Software AS, Oslo, Norway).

2.7. Determination of Antioxidant Activity by the DPPH Method

The antioxidant (free-radical-scavenging) activity of *O. indicum* extracts was determined by the DPPH method with a slight modification from the previous study [26]. Briefly, 20 μL extract samples at various concentrations were added to 200 μL of 0.1 mM DPPH solution in a 96-well plate. The sample tests were incubated in the dark at room temperature for 30 min. Absorbance was measured at 517 nm using a microplate reader (SPECTROstar Nano, BMG LABTECH GmbH, Ortenberg, Germany). Antioxidant activity was expressed as the IC_{50} values, calculated from the dose–response curve of each extract. Ascorbic acid and Trolox were used as positive controls. All experiments were conducted in triplicate.

2.8. Determination of Cytotoxic Activities by the MTT Method

The cytotoxic effects of *O. indicum* extracts on keratinocyte (HaCaT), fibroblast (MRC-5), and macrophage (RAW 264.7) cell lines were evaluated by the MTT method with a slight modification from the previous study [27]. Briefly, HaCaT (1×10^4 cells/mL), MRC-5 (1×10^4 cells/mL), and RAW 264.7 (1×10^5 cells/mL) were seeded in DMEM and incubated for 24 h at 37 °C in a humidified atmosphere containing 5% CO_2. The cells were treated with various concentrations of plant extracts (12.5–200 μg/mL) and further incubated under the same conditions for an additional 24 h. Subsequently, 150 μL of MTT solution (0.5 mg/mL) was added to each well and incubated for 1 h at 37 °C to allow the formation of formazan crystals. After incubation, 100 μL of DMSO was added to dissolve the formazan

product. The absorbance of the resulting solution was measured at 550 nm. Cell viability was expressed as a percentage relative to untreated control cells by comparing their absorbance values. Untreated cells served as the control. All experiments were conducted in triplicate.

2.9. Determination of Anti-Inflammatory Activity by the Inhibition of Nitric Oxide Production

RAW 264.7 cells were stimulated with lipopolysaccharide (LPS; 100 ng/mL) and co-treated with various concentrations of *O. indicum* extracts (12.5–200 μg/mL). The cells were incubated at 37 °C for 24 h. The culture supernatant from each test (0.1 mL) was mixed with an equal volume of Griess reagent (0.1 mL) and incubated at room temperature for 10 min. The absorbance was then measured at 540 nm using a microplate reader. Nitric oxide (NO) production was expressed as a percentage of the control. The NO production of LPS-stimulated cells (100%) was used as the control [28].

2.10. LC-MS/MS Analysis

Phytochemicals in *O. indicum* extracts were characterized using an LC-MS/MS method adapted from a previously reported study [29]. The extract samples (500 ppm) were prepared in absolute methanol, filtered through 0.2 μm nylon (NYL) membrane filters, and transferred into 1.5 mL glass vials. The prepared samples were injected for LC analysis. Chromatographic separation was carried out using an Agilent Poroshell EC-C18 column (2.1 mm × 150 mm, 2.7 μm) coupled with a Poroshell EC-C18 guard column (4.6 mm × 5 mm, 2.7 μm), operated on an Agilent 1290 UHPLC system (Agilent Technologies, Santa Clara, CA, USA). The mobile phases consisted of 0.1% (*v*/*v*) formic acid in water (mobile phase A) and 0.1% (*v*/*v*) formic acid in acetonitrile (mobile phase B), controlled under a gradient elution program at a flow rate of 0.2 mL/min. Mass spectrometric detection was performed using an Agilent G6454B Q-TOF mass spectrometer equipped with a Dual AJS electrospray ionization (ESI) source. The operating parameters included a capillary voltage of 4000 V and a nozzle voltage of 500 V. The skimmer1, fragmentor, and Octopole RF peak voltages were set to 65 V, 150 V, and 750 V, respectively. Data were acquired over an *m*/*z* range of 100–1100 at a scan rate of 1.00 spectra/s. Internal reference masses were applied for real-time mass correction, using *m*/*z* 121.05087300 and 922.00979800 in positive ion mode, and *m*/*z* 112.98558700 and 1033.98810900 in negative ion mode. For tandem MS (MS/MS) analysis, spectra were obtained under the same instrumental conditions as MS acquisition, with collision energies set at 10, 20, and 40 eV.

2.11. Statistical Analysis

Statistical analyses were conducted using IBM SPSS Statistics version 20. Differences among groups were evaluated using analysis of variance (ANOVA). Comparisons between control and treated groups were further assessed using Student's t-test. Statistical significance was defined at a *p*-value of less than 0.05 ($p < 0.05$).

3. Results and Discussion

3.1. Preparation and Extraction Yields of O. indicum

The aerial parts of *O. indicum* were separated into four parts: bark (OB), leaves (OL), pods (OP), and seeds (OS), as illustrated in Figure 1, for subsequent extraction and evaluation of their potential bioactive properties. The fresh bark (OB) typically exhibited a light brownish-gray to yellowish-gray outer surface, while the inner bark layer appeared golden-yellow (Figure 1a). It possessed a spongy, corky, and relatively thick texture. After air-drying, the outer bark color changed to brownish-gray, and the inner layer became grayish yellow (Figure 1b), accompanied by a transition to a slightly rough and scaly

texture. The dried bark was subsequently ground into a fine yellowish-gray powder (Figure 1c). Fresh leaves (OL) were characterized by a deep, glossy green upper surface and a lighter green underside (Figure 1d). The leaves were compound, with pinnate branching and long petioles. After drying, the leaf color shifted to a dull dark green or brownish green, and the texture became brittle and papery (Figure 1e). The resulting leaf powder was fine and appeared light green to pale yellowish-green (Figure 1f). The fresh pods (OP) were elongated, flat, and sword-like in shape, with a smooth and glossy surface (Figure 1g). After drying, the pods turned grayish-brown or yellowish-brown, with a matte, rough surface (Figure 1h). Grinding produced a fine, slightly fluffy powder with a light yellowish-brown color (Figure 1i). Fresh seeds (OS) were small and flat, surrounded by a broad, transparent, papery wing (Figure 1j). After drying, the seeds developed a silvery-white color, while the central portion became matte brown (Figure 1k). The ground seed powder was fine, light, and fluffy, with a very pale yellow coloration (Figure 1l).

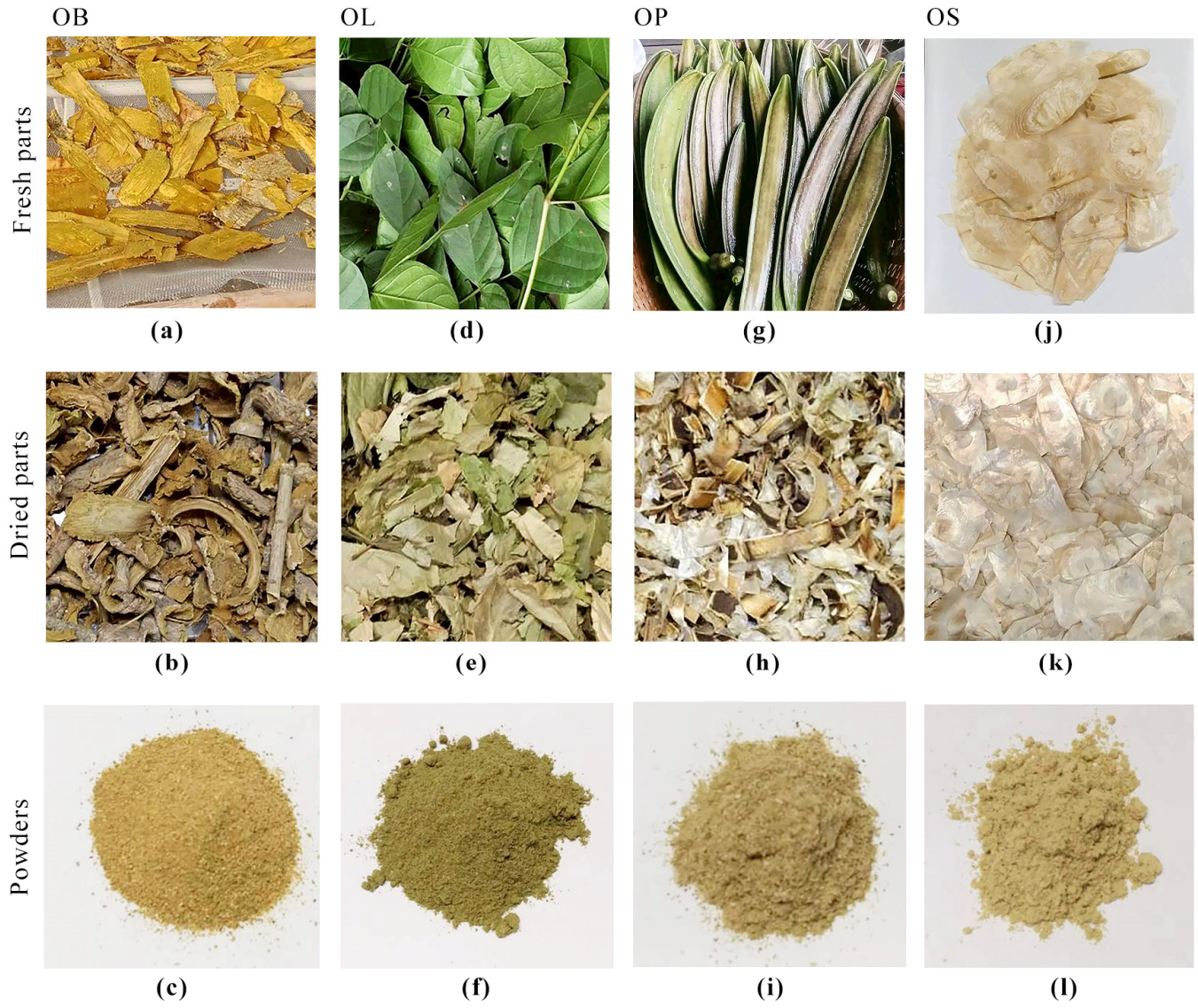


Figure 1. Fresh parts, dried parts, and powders of *Oroxylum indicum*, including bark (OB), leaves (OL), pods (OP), and seeds (OS). (**a**–**c**) Fresh bark, dried bark, and bark powder, respectively; (**d**–**f**) fresh leaves, dried leaves, and leaf powder, respectively; (**g**–**i**) fresh pods, dried pods, and pod powder, respectively; and (**j**–**l**) fresh seeds, dried seeds, and seed powder, respectively.

The crude extract yields of *O. indicum* were obtained using microwave-assisted extraction (MAE). The extracts included MAE-OB50 and MAE-OB70 for the bark (OB), MAE-OL50 and MAE-OL70 for the leaf (OL), MAE-OP50 and MAE-OP70 for the pod (OP), and MAE-OS50 and MAE-OS70 for the seed (OS), obtained from MAE with 50% and 70% (*v*/*v*) ethanol, respectively, as summarized in Table 1. The extraction yields for OB were 34.58 ± 0.68% (MAE-OB50) and 30.80 ± 1.10% (MAE-OB70). For OL, the yields were 33.82 ± 0.98% (MAE-OL50) and 37.42 ± 2.32% (MAE-OL70). OP extracts yielded 16.18 ± 0.49% (MAE-OP50) and 22.07 ± 2.57% (MAE-OP70), while OS extracts yielded 22.06 ± 0.00% (MAE-OS50) and 32.39 ± 1.51% (MAE-OS70). The OB extract obtained with 50% ethanol (MAE-OB50) exhibited a significantly higher yield than that obtained with 70% ethanol (MAE-OB70) ($p < 0.05$). In contrast, no significant differences were observed between the 50% and 70% ethanolic extracts of OL and OP ($p > 0.05$). For the OS extracts, the yield obtained with 70% ethanol (MAE-OS70) was significantly higher than that obtained with 50% ethanol (MAE-OS50) ($p < 0.05$). These results suggest that both solvent composition and plant part significantly influence extraction efficiency. Previous studies have reported that higher ethanol concentrations generally enhance total extract yield compared to aqueous or low-ethanol systems [30] and that extraction yield varies depending on plant part [31]. Consistent with these observations, the present study found that 70% ethanolic extracts of leaves, pods, and seeds generally produced higher yields than their 50% counterparts, whereas bark extraction yielded more extract with 50% ethanol. Notably, statistically significant differences were observed only for bark and seed extracts, while leaf and pod extracts showed comparable yields between the two solvent systems.

Table 1. Extraction yields of *Oroxylum indicum* achieved by MAE.

Crude Extracts	Yield (%)
50% (*v*/*v*) ethanol extraction	
O. indicum's bark (MAE-OB50)	34.58 ± 0.68
O. indicum's leaf (MAE-OL50)	33.82 ± 0.98
O. indicum's pod (MAE-OP50)	16.18 ± 0.49
O. indicum's seed (MAE-OS50)	22.06 ± 0.00
70% (*v*/*v*) ethanol extraction	
O. indicum's bark (MAE-OB70)	30.80 ± 1.10
O. indicum's leaf (MAE-OL70)	37.42 ± 2.32
O. indicum's pod (MAE-OP70)	22.07 ± 2.57
O. indicum's seed (MAE-OS70)	32.39 ± 1.51

Data are reported as mean ± SD ($n = 3$).

3.2. UV–Vis Spectra of the O. indicum Extracts

In this study, the UV–Vis absorption profiles of 50% and 70% ethanolic extracts of *O. indicum* bark, leaf, pod, and seed obtained by MAE are presented in Figure 2. Strong absorption was observed in the short-wavelength UV region (approximately 210–230 nm), accompanied by a distinct absorption band between 270–290 nm, with slight variations depending on the plant part, and a broad, low-intensity shoulder in the 330–360 nm region. The spectra were recorded at a single concentration (100 μg/mL), and some absorbance values were high (approximately 2.5–3.0), particularly in the region below 250 nm, where photometric accuracy may be reduced. Therefore, the spectra are interpreted only qualitatively with respect to the positions of the absorption bands, and the absorbance intensities were not compared among the extracts. This spectral pattern is characteristic of phenolic and flavonoid compounds (240–290 nm), as well as flavones and flavonols (310–370 nm) [32]. The absence of significant absorption beyond 400 nm suggests that the extracts contained UV-active secondary metabolites, such as flavonoids and phenolics,

rather than visible pigments including carotenoids (400–450 nm), anthocyanins (490–550 nm), tannins and terpenoids (400–550 nm), or chlorophylls (600–700 nm) [33]. These results are consistent with previous reports indicating that UV-region absorption peaks are indicative of flavone-type phenolics, which are likely major bioactive constituents of *O. indicum*, such as baicalein [34]. Furthermore, variations in spectral profiles among different plant parts may reflect differences in the composition of specific phytochemicals present in each extract.

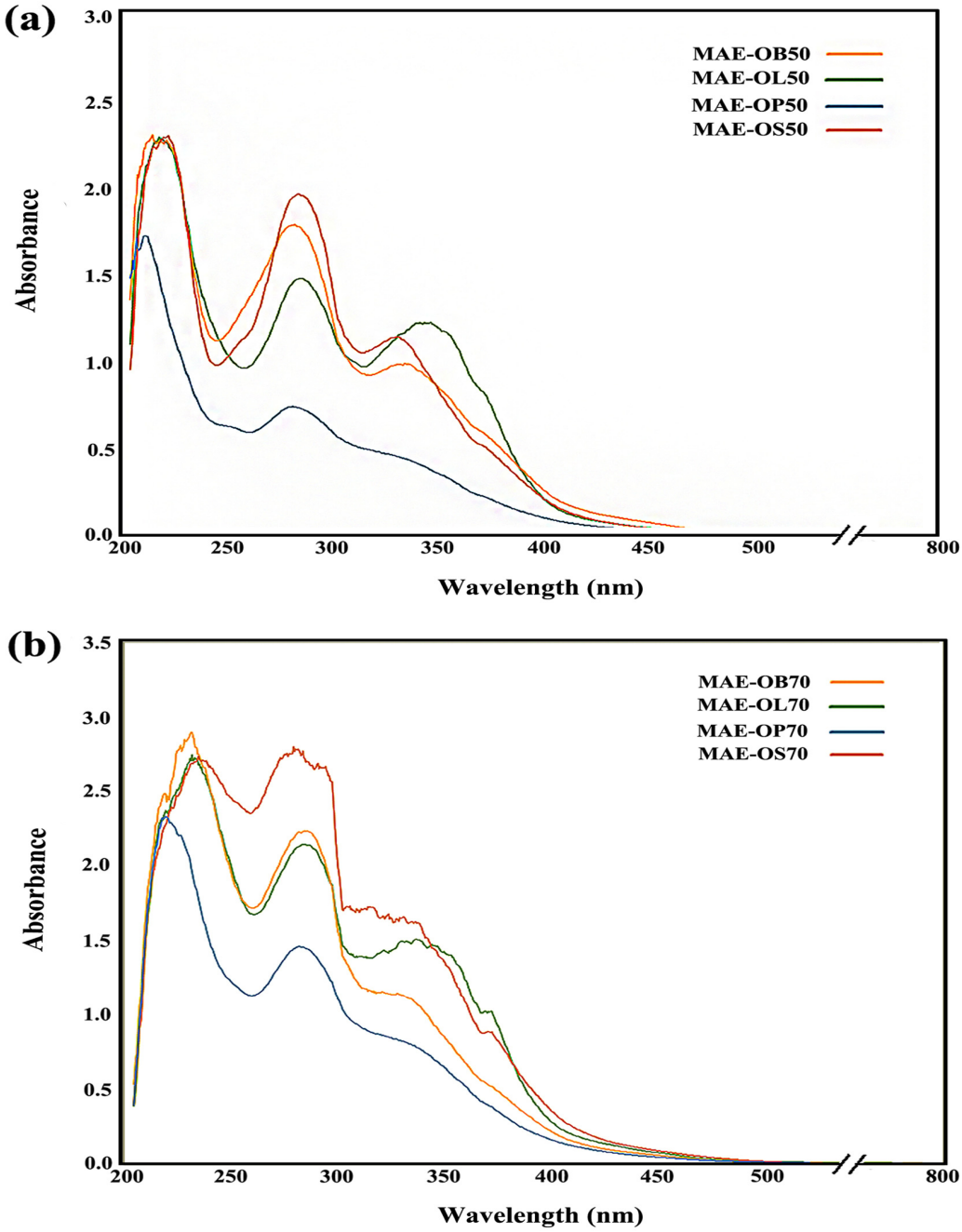


Figure 2. Absorption spectra of the ethanol extracts of *Oroxylum indicum* obtained from MAE were determined by UV–Vis spectrophotometric analysis. UV–Vis spectra of the extracts obtained from 50% (*v*/*v*) ethanol (**a**) and 70% (*v*/*v*) ethanol (**b**) extraction. The 50% ethanol extracts of *O. indicum* bark (MAE-OB50), leaf (MAE-OL50), pod (MAE-OP50), and seed (MAE-OS50). The 70% ethanol extracts of O. *indicum* bark (MAE-OB70), leaf (MAE-OL70), pod (MAE-OP70), and seed (MAE-OS70).

https://doi.org/10.3390/cosmetics13060309

3.3. FTIR Spectra of the O. indicum Extracts

The vibrational spectrum of a chemical compound is regarded as a unique physicochemical characteristic that can provide valuable information on molecular structure and functional groups. The FTIR absorption spectra of dried *O. indicum* extracts recorded within the range of 4000–650 cm^{-1} are presented in Figure 3. Both the 50% ethanolic extracts (Figure 3a) and 70% ethanolic extracts (Figure 3b) exhibited generally similar spectral patterns, particularly within the regions of 3500–1000 cm^{-1}, indicating comparable classes of phytochemical constituents among the extracts. A broad absorption band observed at 3335–3362 cm^{-1} corresponds to O–H stretching vibrations, suggesting the presence of hydroxyl (–OH) groups commonly associated with phenolic compounds, alcohols, or residual moisture. The spectral features are frequently detected in plant extracts rich in flavonoids and phenolic acids [35–37]. The absorption bands at 2853–2929 cm^{-1} were assigned to C–H stretching vibrations of CH_2 and CH_3 groups, characteristic of alkanes and lipid-derived aliphatic compounds present in *O. indicum* extracts [38]. A distinct absorption peak at approximately 1708–1711 cm^{-1} was attributed to non-conjugated C=O stretching vibrations, typically associated with carboxylic acids or ester functionalities [39]. In addition, absorption bands in the range of 1649–1660 cm^{-1} indicated the presence of conjugated aromatic carbonyl groups, commonly found in flavonoids and phenolic acid derivatives [37]. The characteristic peaks at 1606–1613 cm^{-1} were assigned to aromatic C=C stretching vibrations. The C–H bending vibrations were detected at 1450, 1407–1419, and 1360–1369 cm^{-1}. The absorption bands observed at 1051–1074 cm^{-1} corresponded to C–O stretching vibrations, suggesting the presence of carbohydrate- or glycoside-related constituents [39,40]. The results indicate that all *O. indicum* extracts possess structurally complex yet chemically similar compositions, such as flavonoids, phenolic acids, phenolic acid derivatives, alkanes, lipid-derived aliphatic compounds, and carbohydrate- or glycoside-related compounds.

Principal component analysis (PCA) was applied to the FTIR spectral data to evaluate the capability of FTIR spectroscopy in differentiating among the extract samples. The PCA results for the 50% (*v*/*v*) and 70% (*v*/*v*) aqueous ethanolic extracts of *O. indicum* are presented in Figures 4 and 5, respectively. For the 50% (*v*/*v*) ethanolic extracts, the PCA model explained 69% of the total variance, with the first principal component (PC1) accounting for 45% and the second principal component (PC2) accounting for 24% of the variance (Figure 4). As shown in Figure 4a, MAE-OB50 was clearly separated from the other extracts (MAE-OL50, MAE-OP50, and MAE-OS50), indicating distinct chemical characteristics. In Figure 4b, the loading plot of PC1 revealed that the absorption peaks at 1645, 1595, and 1450 cm^{-1} were associated with conjugated aromatic carbonyl (C=O) groups containing high levels of hydroxyl (–OH) or hydrogen substitutions. In addition, the prominent peak observed at 1053 cm^{-1} [41] suggested that MAE-OB50 contained higher amounts of sugars or glycosidic compounds compared to MAE-OL50 and MAE-OS50. In contrast, MAE-OL50 and MAE-OS50 exhibited a dominant C=O absorption peak at 1662 cm^{-1}, indicating a lower degree of conjugation with hydroxyl or hydrogen-substituted aromatic groups. The PCA distribution indicated that MAE-OP50 possessed chemical characteristics intermediate between those of MAE-OB50 and the MAE-OL50/MAE-OS50 groups, suggesting partial similarity in phytochemical composition among these extracts. Furthermore, PC2, which explained 24% of the variance, enabled discrimination between MAE-OB50 and MAE-OL50 from MAE-OP50 and MAE-OS50 (Figure 4c). The latter two extracts (MAE-OP50 and MAE-OS50) exhibited characteristic absorption bands at 2921 and 2852 cm^{-1} [38], corresponding to lipid-related functional groups, indicating a higher contribution of aliphatic or lipid constituents in these extracts.

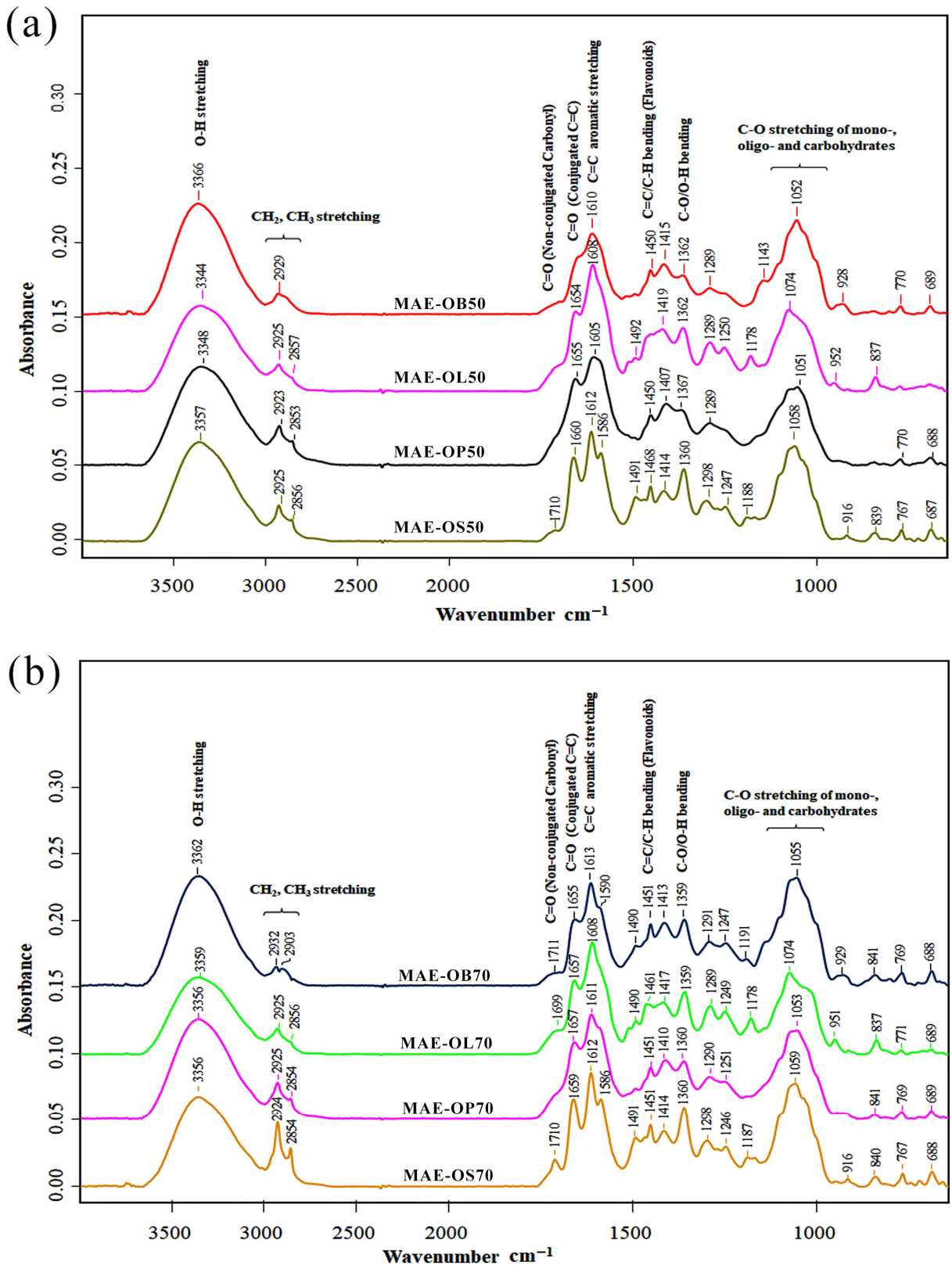


Figure 3. *Oroxylum indicum* extracts obtained from MAE were determined by Fourier Transform Infrared Spectroscopy (FTIR). (**a**) FTIR spectra of the 50% ethanol extracts of *O. indicum* bark (MAE-OB50), leaf (MAE-OL50), pod (MAE-OP50), and seed (MAE-OS50). (**b**) FTIR spectra of the 70% ethanol extracts of *O. indicum* bark (MAE-OB70), leaf (MAE-OL70), pod (MAE-OP70), and seed (MAE-OS70).

For the 70% ethanolic extracts, the PCA model explained 79% of the total variance, with PC1 and PC2 accounting for 59% and 20% of the variance, respectively (Figure 5). As shown in Figure 5a, PC1 clearly differentiated MAE-OL70 from MAE-OB70, MAE-OP70, and MAE-OS70. The loading plot (Figure 5b) showed a dominant absorption peak at nearly 1009 cm^{-1} [42] in MAE-OL70, indicating a relatively higher content of carbohydrate-related compounds compared to the other extracts. In addition, PC2 distinguished MAE-OB70 and portions of MAE-OL70 from MAE-OP70 and MAE-OS70, accounting for 20% of the total variance. In Figure 5c, the MAE-OP70 and MAE-OS70 extracts exhibited more distinct lipid-associated absorption bands at 2921 and 2852 cm^{-1}, [38], indicating a stronger contribution of lipid or aliphatic functional groups in these extracts.

The PCA results collectively suggest that MAE using 50% ethanol was more effective in extracting sugar-, glycoside-, or carbohydrate-related compounds from the bark of *O. indicum* compared to the other plant parts. In contrast, MAE using 70% ethanol appeared to enhance the extraction of these compound groups from the leaves more effectively than from the other parts. Furthermore, lipid- or aliphatic-related compounds were more prominently extracted from the pods and seeds than from the bark or leaves under both 50% and 70% ethanolic MAE conditions.

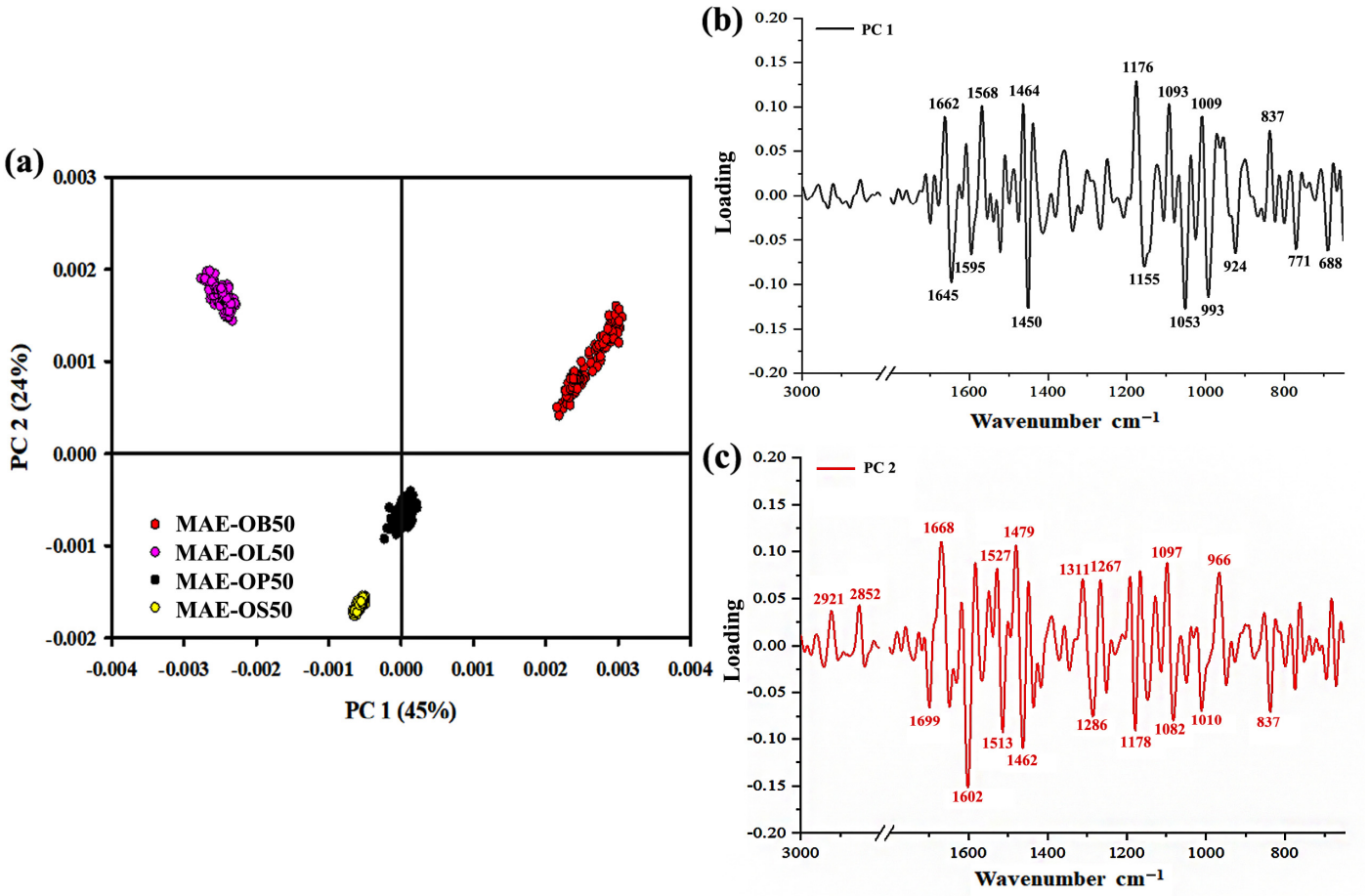


Figure 4. *Oroxylum indicum* extracts obtained from MAE with 50% (*v*/*v*) ethanol were determined by PCA. PCA score plot (**a**). Loading plot: PC1 (**b**) and PC2 (**c**) of *O. indicum* extracts. The 50% ethanol extracts of *O. indicum* bark (MAE-OB50), leaf (MAE-OL50), pod (MAE-OP50), and seed (MAE-OS50).

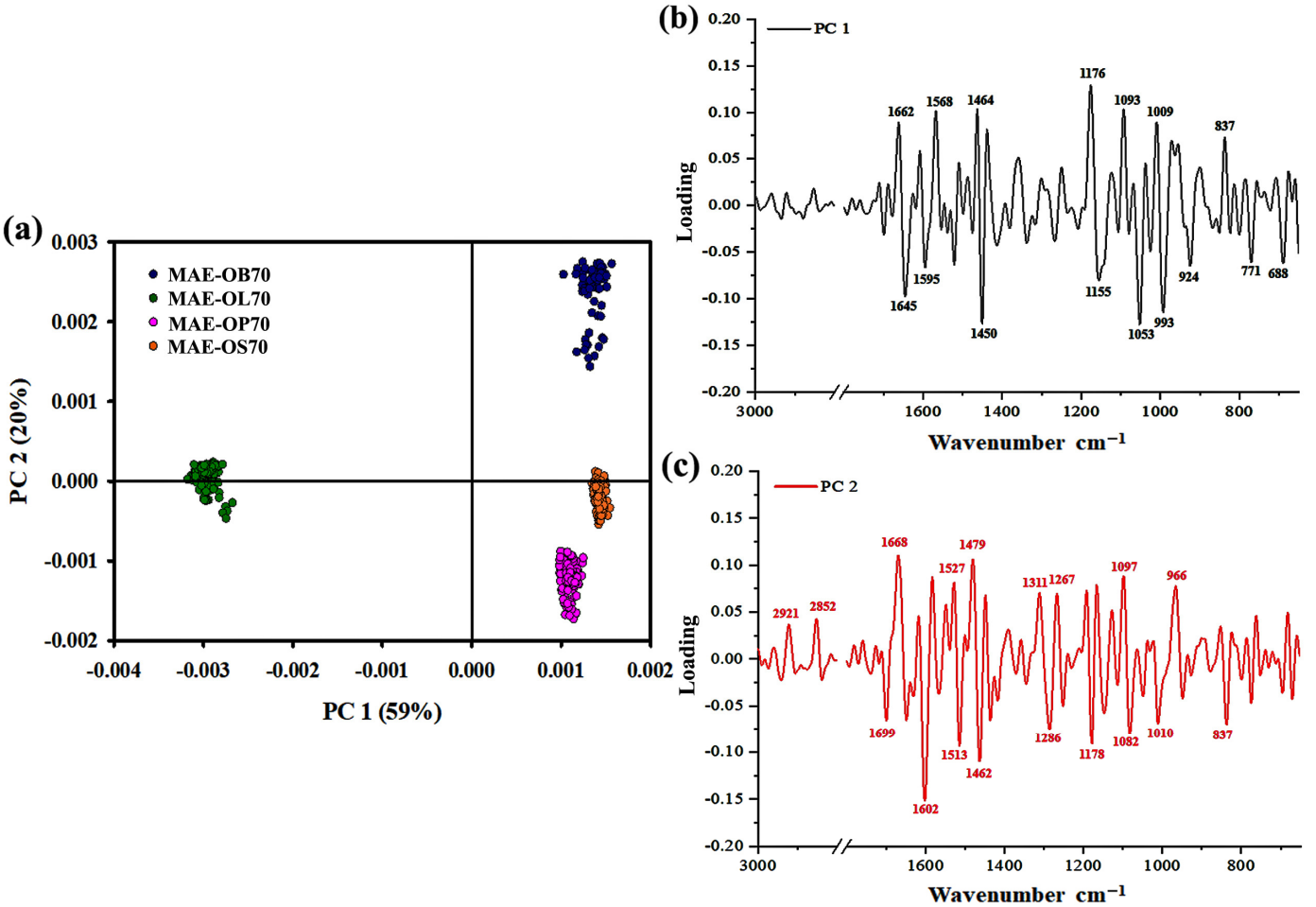


Figure 5. *Oroxylum indicum* extracts obtained from MAE with 70% (*v*/*v*) ethanol were analyzed by PCA. PCA score plot (**a**). Loading plot: PC1 (**b**) and PC2 (**c**) of *O. indicum* extracts. The 70% ethanol extracts of *O. indicum* bark (MAE-OB70), leaf (MAE-OL70), pod (MAE-OP70), and seed (MAE-OS70).

3.4. Antioxidant Activity of O. indicum Extracts

The antioxidant capacity (free-radical-scavenging activity) of *O. indicum* extracts was evaluated using the DPPH radical scavenging assay. Ascorbic acid and Trolox were used as positive controls, exhibiting IC_{50} values of 0.08 ± 0.00 mg/mL and 0.03 ± 0.00 mg/mL, respectively. As presented in Table 2, the IC_{50} values of the bark extracts, MAE-OB50 and MAE-OB70, were 1.04 ± 0.08 mg/mL and 0.49 ± 0.12 mg/mL, respectively. MAE-OB70 exhibited significantly stronger antioxidant activity than MAE-OB50 ($p < 0.05$). The leaf extracts, MAE-OL50 and MAE-OL70, showed IC_{50} values of 0.54 ± 0.04 mg/mL and 0.45 ± 0.15 mg/mL, respectively. No significant difference was observed between the antioxidant activities of MAE-OL50 and MAE-OL70 ($p > 0.05$). For the pod extracts, MAE-OP50 and MAE-OP70 exhibited IC_{50} values of 1.06 ± 0.15 mg/mL and 0.50 ± 0.17 mg/mL, respectively. MAE-OP70 showed significantly greater antioxidant activity compared to MAE-OP50 ($p < 0.05$). The seed extracts, MAE-OS50 and MAE-OS70, demonstrated IC_{50} values of 0.40 ± 0.04 mg/mL and 0.35 ± 0.06 mg/mL, respectively. The antioxidant activities of the seed extracts (MAE-OS50 and MAE-OS70) were not significantly different ($p > 0.05$). The IC_{50} values of the extracts were markedly higher than those of ascorbic acid and Trolox, reflecting the expected lower antioxidant potency of crude plant extracts compared to purified reference compounds. Among all extracts tested, the seed extracts, particularly MAE-OS50 and MAE-OS70, demonstrated the strongest antioxidant activity. A study by Nigam

et al. (2025) similarly reported variations in antioxidant activity among different plant parts, showing that leaf extracts exhibited stronger antioxidant activity than stem bark, root bark, and root extracts, respectively [43]. Sithisarn et al. (2016) reported that ethanolic seed extracts exhibited markedly greater antioxidant activity than ethanolic fruit extracts, while ethanol maceration consistently produced higher antioxidant activity than aqueous decoction for both seeds and fruits [44]. Collectively, these findings support the present results, indicating that both the extraction solvent and the plant part play critical roles in determining the antioxidant potential of *O. indicum* extracts, as reflected by the differences in DPPH IC_{50} values.

Table 2. Antioxidant activity, cytotoxic activity (cell viability), and anti-inflammatory activity of *Oroxylum indicum* extracts, achieved by MAE.

Extracts	Antioxidant Activity Against DPPH Radicals IC_{50} (mg/mL)	Cell Viability by MTT Assays at 200 μg/mL of the Extracts (%)			Anti-Inflammatory Activity Against NO Production IC_{50} (μg/mL)
		HaCaT	MRC-5	RAW 264.7	
MAE-OB50	1.04 ± 0.08	69.96 ± 3.07	101.86 ± 6.09	96.47 ± 1.27	>200
MAE-OL50	0.54 ± 0.04	82.31 ± 5.30	71.75 ± 2.44	119.37 ± 1.07	128.00 ± 2.80
MAE-OP50	1.06 ± 0.15	106.65 ± 9.07	131.72 ± 2.27	99.83 ± 1.24	>200
MAE-OS50	0.40 ± 0.04	73.12 ± 1.24	62.58 ± 2.48	104.08 ± 1.35	>200
MAE-OB70	0.49 ± 0.12	94.95 ± 7.51	87.42 ± 9.06	116.39 ± 1.62	178.72 ± 3.52
MAE-OL70	0.45 ± 0.15	85.25 ± 4.45	90.69 ± 4.69	118.94 ± 3.18	126.26 ± 0.71
MAE-OP70	0.50 ± 0.17	116.79 ± 12.53	119.50 ± 9.43	115.80 ± 1.05	>200
MAE-OS70	0.35 ± 0.06	77.79 ± 5.23	91.32 ± 7.74	118.49 ± 0.24	147.03 ± 0.59
Ascorbic acid	0.08 ± 0.00	NA	NA	NA	NA
Trolox	0.03 ± 0.00	NA	NA	NA	NA

All data are reported as mean ± SD (n = 3). NA, not applicable.

3.5. In Vitro Cytotoxic Activities of O. indicum Extracts

The cytotoxic effects of *O. indicum* extracts were evaluated using human keratinocyte HaCaT, human fibroblast MRC-5, and murine macrophage RAW 264.7 cells by MTT assay. Untreated cells were considered to be the control group and defined as 100% cell viability. The cytotoxic activities of the 50% and 70% aqueous ethanolic extracts are expressed as percentages of cell viability, as summarized in Table 2. For HaCaT cells, the cell viabilities of MAE-OB50, MAE-OL50, and MAE-OS50 at 200 μg/mL were 69.96 ± 3.07%, 82.31 ± 5.30%, and 73.12 ± 1.24%, respectively, whereas MAE-OP50 exhibited a cell viability of 106.65 ± 9.07%. Similarly, the cell viabilities of MAE-OB70, MAE-OL70, and MAE-OS70 were 94.95 ± 7.51%, 85.25 ± 4.45%, and 77.79 ± 5.23%, respectively, while MAE-OP70 showed a viability of 116.79 ± 12.53%. Notably, MAE-OB50 and MAE-OS50 reduced HaCaT cell viability to approximately 70% and 73%, respectively, suggesting appreciable cytotoxic effects at the tested concentration. In contrast, both pod extracts maintained cell viability above 100%, indicating no apparent reduction in cell viability under these experimental conditions. For MRC-5 cells, the cell viabilities of MAE-OL50 and MAE-OS50 were 71.75 ± 2.44% and 62.58 ± 2.48%, respectively, while MAE-OB50 and MAE-OP50 exhibited viabilities of 101.86 ± 6.09% and 131.72 ± 2.27%, respectively. The cell viabilities of MAE-OB70, MAE-OL70, and MAE-OS70 were 87.42 ± 9.06%, 90.69 ± 4.69%, and 91.32 ± 7.74%, respectively, whereas MAE-OP70 demonstrated a viability of 119.50 ± 9.43%. Among the tested extracts, MAE-OS50 produced the greatest reduction in MRC-5 cell viability, reaching approximately 63% at 200 μg/mL. MAE-OL50 also caused a notable reduction in cell viability, whereas the remaining extracts exhibited relatively smaller effects. These findings indicate that the cytotoxic responses varied depending on the plant

part, extraction conditions, and cell type. For RAW 264.7 macrophage cells, the cell viabilities of MAE-OB50, MAE-OL50, MAE-OP50, and MAE-OS50 were 96.47 ± 1.27%, 119.37 ± 1.07%, 99.83 ± 1.24%, and 104.08 ± 1.35%, respectively. In addition, MAE-OB70, MAE-OL70, MAE-OP70, and MAE-OS70 showed cell viabilities of 116.39 ± 1.62%, 118.94 ± 3.18%, 115.80 ± 1.05%, and 118.49 ± 0.24%, respectively. These results indicate that none of the tested extracts caused an appreciable reduction in RAW 264.7 cell viability under the experimental conditions.

Previous studies have demonstrated the safety profiles of *O. indicum* extracts in various cell models. Abdulhafiz et al. (2022) reported that leaf extracts prepared by maceration with 95% ethanol exhibited wound-healing activity by promoting the migration of HaCaT cells at concentrations of 25 and 50 μg/mL, indicating that the extract was non-toxic to the cells at these concentrations [45]. In addition, bark extracts of *O. indicum* were reported to be safe for human lung fibroblast (WI-38) cells at concentrations ranging from 50–100 μg/mL, but exhibited dose-dependent cytotoxicity at higher concentrations between 200 and 1000 μg/mL [46]. Furthermore, Dunkhunthod et al. (2020) demonstrated that pod extracts prepared by Soxhlet extraction with 95% ethanol did not affect the viability of RAW 264.7 cells at concentrations below 300 μg/mL [47]. These findings are generally consistent with the present results, particularly the relatively high cell viability observed following treatment with pod extracts and the reductions in cell viability induced by certain bark, leaf, and seed extracts at 200 μg/mL. Overall, the findings suggest that the in vitro cytocompatibility of *O. indicum* extracts depends on the plant part, extraction conditions, concentration, and cell type. Nevertheless, the present results are preliminary and do not establish cosmetic safety. Further investigations, including skin irritation, sensitization, and comprehensive toxicological assessments, are required to evaluate their suitability for cosmetic applications.

3.6. Anti-Inflammatory Activity of O. indicum Extracts

The anti-inflammatory activities of *O. indicum* extracts were evaluated by NO inhibition in LPS-stimulated RAW 264.7 macrophages, as presented in Table 2. Among the tested extracts, MAE-OL50, MAE-OB70, MAE-OL70, and MAE-OS70 demonstrated inhibitory effects on NO production, with IC_{50} values of 128.00 ± 2.80, 178.72 ± 3.52, 126.26 ± 0.71, and 147.03 ± 0.59 μg/mL, respectively. In contrast, the remaining extracts exhibited no significant anti-inflammatory activity (IC_{50} > 200 μg/mL). Among the different plant parts, leaf extracts prepared with both 50% and 70% ethanol exhibited the greatest inhibitory potency, followed by the 70% ethanolic extracts of seed and bark. Moreover, the extracts obtained using 70% ethanol extraction generally showed lower IC_{50} values than those extracted with 50% ethanol extraction, indicating stronger anti-inflammatory activity. However, ethanolic leaf extracts of *O. indicum* have been reported to exhibit stronger inhibitory effects on NO production than pod extracts, supporting the influence of plant part on anti-inflammatory potential [47]. In addition, Rodwattanagul et al. (2025) [18] demonstrated that stem bark extracts prepared using different solvents, including hexane, ethyl acetate, and ethanol, showed varying degrees of anti-inflammatory activity. Thus, the present results indicate that both extraction solvent and plant part are critical factors influencing the anti-inflammatory efficacy of *O. indicum* extracts, as reflected by differences in their IC_{50} values.

3.7. LC-MS/MS Analysis of O. indicum Extracts

The phytochemical profiles of *O. indicum* extracts, including MAE-OL50, MAE-OL70, MAE-OB70, and MAE-OS70, were investigated using LC-QTOF-MS/MS-based tentative identification. Compound annotation was performed based on several selection criteria, including relative peak intensity (percentage height) from the LC-MS chromatograms

(Figure 6), retention time, mass accuracy with a mass error tolerance of −5 to 5 ppm (DB Diff), match score ≥ 90%, MS ions in the negative ionization mode ($[M-H]^-$), molecular formula, and MS/MS fragment ions. The tentative identification results for MAE-OL50, MAE-OL70, MAE-OB70, and MAE-OS70 are presented in Tables 3–6, respectively, with corresponding supplementary information provided in Tables S1–S4.

According to Table 3, a total of 24 compounds were tentatively identified in MAE-OL50, consisting predominantly of flavonoid glycosides and conjugated derivatives. The major constituents identified in MAE-OL50 included quercetin, pinoquercetin, kaempferol-3-*O*-galactoside, baicalin, oroxindin, diosmetin 7-*O*-β-D-glucuronopyranoside, quercetin 3-methyl ether 7-glucuronide, and isoacteoside. In addition, 6-gingerol and naringin dihydrochalcone were found in this extract. The high abundance of glucuronidated and glycosylated flavonoids suggests that MAE-OL50 contains relatively polar phytochemical constituents, which may contribute to improved aqueous solubility and enhanced biological availability of the bioactive compounds.

A total of 27 compounds were tentatively identified in MAE-OL70 (Table 4). Similar to MAE-OL50, MAE-OL70 exhibited a high diversity of flavonoid derivatives, particularly glucuronidated and methoxylated flavones. The major compounds identified in this extract included pyroglutamic acid, prunetin, luteolin 7-methyl ether, daidzein 8-C-glucoside, apigenin 7-*O*-glucuronide, scutellarein 7-glucuronide, tectoridin, verbascoside, and isorhamnetin 3-*O*-glucoside. In addition, kaempferol derivatives and flavone glycosides were abundantly found in the extract. The presence of both methylated flavonoids and glycosylated conjugates suggests that MAE-OL70 has a balanced composition of hydrophilic and moderately lipophilic phytochemicals, which may contribute to diverse biological activities and improved extraction efficiency using 70% ethanol.

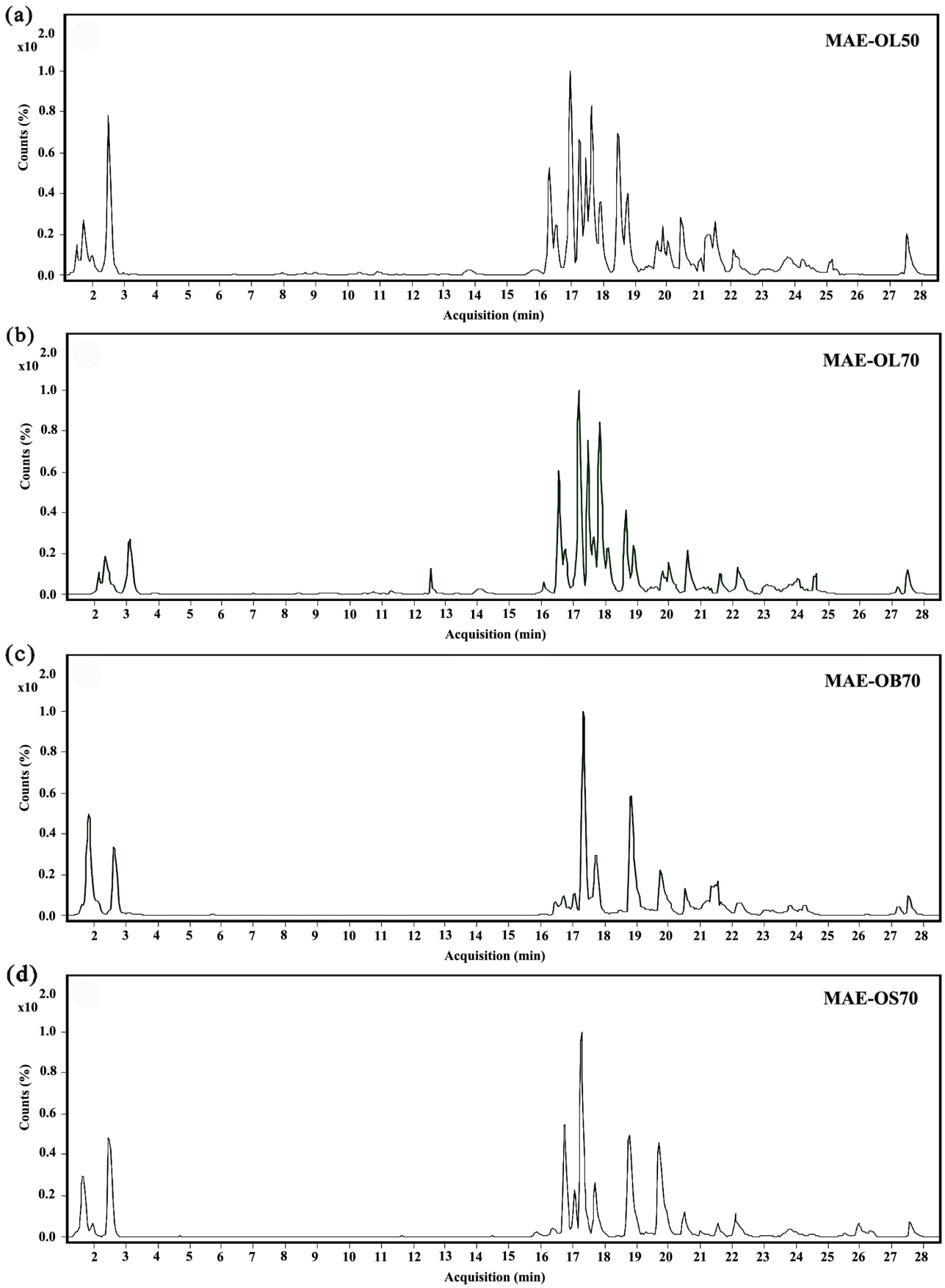


Figure 6. LC chromatograms of *Oroxylum indicum* extracts obtained from the LC-MS/MS analysis. The chromatograms of MAE-OL50 (**a**), MAE-OL70 (**b**), MAE-OB70 (**c**), and MAE-OS70 (**d**).

Table 5 shows that a total of 25 compounds were tentatively identified in MAE-OB70. The phytochemical profile of MAE-OB70 exhibited a distinct pattern, characterized predominantly by methoxylated flavones and flavonoid glucuronides. The major compounds tentatively identified in this extract included baicalein, oroxylin A, diosmetin, acacetin, chrysin 7-*O*-β-D-glucuronide, oroxylin A glucuronide, luteolin 7-*O*-glucuronide, cupressuflavone, magnoloside A, and stachyose. Methoxylated flavones such as oroxylin A, diosmetin, and acacetin are recognized for their enhanced lipophilicity. The predominance of these compounds suggests that the extraction conditions applied to the *O. indicum* bark favored the recovery of relatively less polar flavonoids and conjugated phenolic constituents.

A total of 22 compounds were tentatively identified in MAE-OS70, as presented in Table 6. Among all extracts, MAE-OS70 exhibited the largest number of tentatively identified isoflavones and carbohydrate-associated constituents. Representative compounds identified in this extract included apigenin, daidzein, genistein, trehalose, raffinose, guaijaverin, homoplantaginin, nicotiflorin, rhoifolin, and daidzein 8-C-glucoside. Isoflavones such as daidzein and genistein are well-recognized phytoestrogenic compounds with potent antioxidant properties [48]. In addition, the recognition of sugar-related constituents, including trehalose and raffinose, suggests that MAE-OS70 contains a relatively higher proportion of hydrophilic constituents compared with the other extracts.

The comparative LC-MS profiling suggested differences in the tentatively identified compounds among the O. *indicum* extracts. The bark extract (MAE-OB70) was characterized by the detection of several methoxylated flavones and bioactive phenolic conjugates, whereas the leaf extract (MAE-OL50 and MAE-OL70) exhibited a broader diversity of flavonoid glycosides and glucuronides. In contrast, the seed extract (MAE-OS70) was distinguished primarily by the presence of isoflavones and sugar-associated constituents. The LC-MS/MS tentative identification further indicates that the *O. indicum* extracts are rich sources of flavonoids and flavonoid conjugates with previously reported antioxidant and anti-inflammatory properties, consistent with previous studies employing maceration and ultrasonication extraction methods [17,21]. Several compounds identified in the extracts, particularly luteolin [49,50], apigenin [50], baicalein [51], quercetin [50,52], and oroxylin A [53], have been reported to inhibit nitric oxide (NO) production in activated macrophages through suppression of inducible nitric oxide synthase (iNOS) expression and modulation of NF-κB signaling pathways. Therefore, the biological activities observed in the present study, especially the inhibition of NO production in macrophages, are likely to be associated with the synergistic effects of multiple flavonoids and phenolic constituents rather than the activity of a single compound alone. Among the investigated extracts, the extracts of *O. indicum* bark (MAE-OB70) and leaf (MAE-OL50 and MAE-OL70) appeared to be particularly enriched in anti-inflammatory flavonoids, whereas its seed extract (MAE-OS70) contained relatively higher levels of isoflavones and antioxidant glycosides.

Table 3. Tentative identification of phytochemical constituents in the 50% (*v*/*v*) ethanol extract of *Oroxylum indicum* leaf (MAE-OL50) performed via LC-QTOF-MS/MS in negative mode.

No.	RT (min)	Formula	*m*/*z*	Mass Error	Compound	Chemical Classification
1	1.986	$C_8H_{14}O_7$	221.0661	3.06	Ethyl glucuronide	Glucuronide conjugate
2	16.287	$C_{21}H_{20}O_{11}$	447.0926	1.57	Kaempferol 3-*O*-galactoside	Flavonol glycoside
3	16.321	$C_{29}H_{36}O_{15}$	623.1976	−0.87	Isoacteoside	Phenylpropanoid glycoside
4	16.333	$C_{21}H_{18}O_{12}$	461.0720	0.86	Scutellarein 7-glucuronide	Flavone glucuronide
5	16.518	$C_{22}H_{22}O_{12}$	477.1023	−3.25	Isorhamnetin 3-*O*-glucoside	Flavonol glycoside

6	16.539	$C_{22}H_{20}O_{13}$	491.0818	2.75	Quercetin 3-methyl ether 7-glucuronide	Methylated flavonol glucuronide
7	16.814	$C_{21}H_{20}O_{9}$	415.1028	1.29	Daidzein 8-C-glucoside	Isoflavone C-glycoside
8	16.872	$C_{15}H_{10}O_{7}$	301.0340	4.76	Quercetin	Flavonol
9	16.979	$C_{22}H_{20}O_{12}$	475.0863	2.69	5,7,2′-Trihydroxy-8-methoxyflavone 7-glucuronide	Methoxylated flavone glucuronide
10	17.242	$C_{27}H_{34}O_{14}$	581.1855	3.78	Naringin dihydrochalcone	Dihydrochalcone flavonoid
11	17.260	$C_{21}H_{20}O_{10}$	431.0973	2.65	Apigenin 7-*O*-glucoside	Flavone glycoside
12	17.268	$C_{15}H_{10}O_{5}$	269.0454	0.55	Apigenin	Flavone
13	17.269	$C_{21}H_{18}O_{11}$	445.0779	−0.32	Baicalin	Flavone glucuronide
14	17.293	$C_{30}H_{26}O_{13}$	593.1303	−0.19	Kaempferol 3-(2″-p-coumarylglucoside)	Acylated flavonol glycoside
15	17.403	$C_{22}H_{20}O_{12}$	475.0874	1.76	Diosmetin 7-*O*-β-D-glucuronopyranoside	Flavone glucuronide
16	17.464	$C_{15}H_{10}O_{6}$	285.0405	−0.24	Luteolin	Flavone
17	17.638	$C_{22}H_{20}O_{11}$	459.0908	4.9	Oroxindin	Flavone glycoside
18	17.702	$C_{21}H_{18}O_{10}$	429.0807	4.73	Chrysin 7-*O*-β-D-glucuronide	Flavone glucuronide
19	17.888	$C_{15}H_{10}O_{6}$	285.0402	0.95	5,7,2′,6′-Tetrahydroxyflavone	Polyhydroxylated flavone
20	17.926	$C_{16}H_{12}O_{7}$	315.0503	1.99	Pinoquercetin	Flavanonol
21	19.687	$C_{15}H_{10}O_{4}$	253.0503	1.25	Chrysin	Flavone
22	19.793	$C_{17}H_{26}O_{4}$	293.1757	0.65	6-Gingerol	Phenolic ketone
23	19.876	$C_{16}H_{12}O_{5}$	283.0609	1.09	Acacetin	Methoxylated flavone
24	20.468	$C_{10}H_{13}NO_{3}$	194.0818	2.5	*n*-acetyldopamine	Phenolic amide

Note: RT = retention time.

Table 4. Tentative identification of phytochemical constituents in the 70% (*v*/*v*) ethanol extract of *Oroxylum indicum* leaf (MAE-OL70) performed via LC-QTOF-MS/MS in negative mode.

No.	RT (min)	Formula	*m*/*z*	Mass Error	Compound	Chemical Classification
1	2.423	$C_{5}H_{7}NO_{3}$	128.0351	2.11	Pyroglutamic acid	Amino acid derivative
2	2.501	$C_{8}H_{14}O_{7}$	221.0662	1.63	Ethyl glucuronide	Glucuronide conjugate
3	16.290	$C_{21}H_{20}O_{11}$	447.0932	0.17	Kaempferol 3-*O*-galactoside	Flavonol glycoside
4	16.322	$C_{29}H_{36}O_{15}$	623.1959	−3.60	Verbascoside	Phenylpropanoid glycoside
5	16.333	$C_{21}H_{18}O_{12}$	461.0722	1.11	Scutellarein 7-glucuronide	Flavone glycoside
6	16.526	$C_{22}H_{22}O_{12}$	477.1019	−1.78	Isorhamnetin 3-*O*-glucoside	Flavonol glycoside
7	16.543	$C_{22}H_{20}O_{13}$	491.0830	0.42	Carminic acid	Anthraquinone glycoside
8	16.815	$C_{21}H_{20}O_{9}$	415.1023	2.7	Daidzein 8-C-glucoside	Isoflavone C-glycoside
9	16.906	$C_{21}H_{18}O_{11}$	445.0772	0.98	Baicalin	Flavone glucuronide
10	16.916	$C_{22}H_{22}O_{11}$	461.1089	0.21	Tectoridin	Isoflavone glycoside
11	16.980	$C_{22}H_{20}O_{12}$	475.0881	−0.27	5,7,2′-Trihydroxy-8-methoxyflavone 7-glucuronide	Methoxylated flavone glucuronide
12	16.982	$C_{16}H_{12}O_{6}$	299.057	−2.63	Luteolin 7-methyl ether	Methoxylated flavone
13	16.986	$C_{21}H_{24}FIN_{2}O_{3}$	497.0704	4.47	2,3-Dimethoxy-5-iodo-*N*-((1-(4′-fluorobenzyl)-2-pyrrolidinyl)methyl)benzamide	Benzamide derivative
14	17.237	$C_{27}H_{34}O_{14}$	581.1855	3.71	Naringin dihydrochalcone	Dihydrochalcone flavonoid

15	17.269	$C_{15}H_{10}O_5$	269.0454	0.64	Apigenin	Flavone
16	17.269	$C_{21}H_{18}O_{11}$	445.0763	2.48	Apigenin 7-*O*-glucuronide	Flavone glucuronide
17	17.295	$C_{30}H_{26}O_{13}$	593.1307	−0.9	Kaempferol 3-(2″-p-coumarylglucoside)	Acylated flavonol glycoside
18	17.402	$C_{22}H_{20}O_{12}$	475.0861	4.56	Diosmetin 7-*O*-β-D-glucuronopyranoside	Flavone glucuronide
19	17.466	$C_{15}H_{10}O_6$	285.0392	4.52	Luteolin	Flavone
20	17.637	$C_{22}H_{20}O_{11}$	459.0912	3.9	Oroxindin	Flavone glycoside
21	17.639	$C_{16}H_{12}O_5$	283.061	0.55	Prunetin	Methoxylated isoflavone
22	17.703	$C_{21}H_{18}O_{10}$	429.0817	2.51	Chrysin 7-*O*-β-D-glucuronide	Flavone glucuronide
23	17.887	$C_{15}H_{10}O_6$	285.0401	1.34	5,7,2′,6′-Tetrahydroxyflavone	Polyhydroxylated flavone
24	17.924	$C_{16}H_{12}O_7$	315.0501	2.39	Pinoquercetin	Flavanonol
25	18.403	$C_{15}H_{10}O_5$	269.046	−0.97	Genistein	Isoflavone
26	19.690	$C_{15}H_{10}O_4$	253.0498	3.32	Chrysin	Flavone
27	20.477	$C_{10}H_{13}NO_3$	194.0818	2.17	*n*-acetyldopamine	Phenolic amide

Note: RT = retention time.

Table 5. Tentative identification of phytochemical constituents in the 70% (*v*/*v*) ethanol extract of *Oroxylum indicum* bark (MAE-OB70) performed via LC-QTOF-MS/MS in negative mode.

No.	RT (min)	Formula	*m*/*z*	Mass Error	Compound	Chemical Classification
1	1.603	$C_2HF_3O_2$	112.9856	0.19	Trifluoroacetic acid	Organic acid
2	1.669	$C_{24}H_{42}O_{21}$	665.2146	0.02	Stachyose	Oligosaccharide
3	1.753	$C_{12}H_{22}O_{11}$	377.0874	−4.54	Sucrose	Disaccharide
4	2.525	$C_8H_{14}O_7$	221.0669	−1.27	Ethyl glucuronide	Glucuronide conjugate
5	16.391	$C_{29}H_{36}O_{15}$	623.1982	0.23	Magnoloside A	Polyphenolic glycoside
6	16.434	$C_{21}H_{18}O_{12}$	461.0733	−2.50	Luteolin 7-*O*-glucuronide	Flavone glucuronide
7	16.563	$C_{27}H_{30}O_{13}$	561.1620	−1.15	6,8-Di-C-rhamnosylapigenin	C-glycosyl flavone
8	16.657	$C_{26}H_{28}O_{13}$	547.1466	−1.47	Chrysin 6-C-alpha-L-arabinopyranoside-8-C-glucoside	Di-C-glycosyl flavone
9	16.861	$C_{21}H_{20}O_9$	415.1033	0.99	Daidzein 8-C-glucoside	Isoflavone C-glycoside
10	17.016	$C_{22}H_{24}N_6O_{11}$	547.144	−2.16	2,4,6-Trinitrophenyl-tyrosyl-valyl-glycine	Peptide derivative
11	17.251	$C_{27}H_{34}O_{14}$	581.1855	3.70	Naringin dihydrochalcone	Dihydrochalcone flavonoid
12	17.272	$C_{21}H_{20}O_{10}$	431.0973	2.71	Apigenin 7-*O*-glucoside	Flavone glycoside
13	17.295	$C_{15}H_{10}O_5$	269.0448	2.59	Apigenin	Flavone
14	17.519	$C_{15}H_{10}O_6$	285.0407	−0.88	Luteolin	Flavone
15	17.650	$C_{22}H_{20}O_{11}$	459.0922	2.63	Oroxylin A glucuronide	Methoxylated flavone conjugate
16	17.651	$C_{16}H_{12}O_5$	283.0607	1.57	Oroxylin A	O-methylated flavone
17	17.718	$C_{15}H_{10}O_4$	253.0505	0.63	Daidzein	Isoflavone
18	17.720	$C_{21}H_{18}O_{10}$	429.0809	3.90	Chrysin 7-*O*-β-D-glucuronide	Flavone glucuronide
19	18.525	$C_{16}H_{12}O_6$	299.0559	0.83	Diosmetin	Methoxylated flavone
20	18.796	$C_{15}H_{10}O_5$	269.0453	0.98	Baicalein	Flavone
21	19.194	$C_{30}H_{18}O_{10}$	537.0815	2.35	Cupressuflavone	Biflavonoid
22	19.734	$C_{15}H_{10}O_4$	253.0507	−0.09	Chrysin	Flavone
23	19.810	$C_{17}H_{26}O_4$	293.1755	1.28	6-Gingerol	Phenolic ketone
24	19.926	$C_{16}H_{12}O_5$	283.0613	−0.29	Acacetin	Methoxylated flavone

25	20.507	$C_{10}H_{13}NO_3$	194.0822	0.33	*n*-acetyldopamine	Phenolic amide

Note: RT = retention time.

Table 6. Tentative identification of phytochemical constituents in the 70% (*v*/*v*) ethanol extract of *Oroxylum indicum* seed (MAE-OS70) performed via LC-QTOF-MS/MS.

No.	RT (min)	Formula	*m*/*z*	Mass Error	Compound	Chemical Classification
1	1.676	$C_{18}H_{32}O_{16}$	503.1612	1.30	Raffinose	Oligosaccharide
2	1.738	$C_{12}H_{22}O_{11}$	341.1072	4.67	Trehalose	Disaccharide
3	2.514	$C_8H_{14}O_7$	221.0663	0.79	Ethyl glucuronide	Glucuronide conjugate
4	15.887	$C_{26}H_{28}O_{13}$	547.1433	−4.43	Chrysin 6-C-glucoside-8-C-alpha-L-arabinopyranoside	Di-C-glycosyl flavone
5	16.342	$C_{21}H_{20}O_{11}$	447.0942	−1.7	Kaempferol 3-*O*-galactoside	Flavonol glycoside
6	16.426	$C_{26}H_{28}O_{13}$	547.1432	−4.61	Chrysin 6-C-α-L-arabinopyranoside-8-C-glucoside	Di-C-glycosyl flavone
7	16.665	$C_{20}H_{18}O_{11}$	433.0774	0.64	Guaijaverin	Flavonol glycoside
8	16.746	$C_{27}H_{30}O_{15}$	593.1506	1.19	Nicotiflorin	Flavonol O-glycosides
9	16.747	$C_{15}H_{10}O_5$	269.0457	−0.55	Genistein	Isoflavone
10	16.824	$C_{21}H_{20}O_9$	415.1026	2.15	Daidzein 8-C-glucoside	Isoflavone C-glycoside
11	17.059	$C_{15}H_{10}O_4$	253.0499	3.27	Daidzein	Isoflavone
12	17.059	$C_{28}H_{32}O_{16}$	623.1621	0.79	Narcissin	Flavonol glycoside
13	17.061	$C_{27}H_{30}O_{14}$	577.1537	4.40	Rhoifolin	Flavone glycoside
14	17.265	$C_{21}H_{20}O_{10}$	431.0972	2.9	Apigenin 7-*O*-glucoside	Flavone glycoside
15	17.390	$C_{22}H_{22}O_{11}$	461.1081	1.96	Homoplantaginin	Methoxylated flavone conjugate
16	17.481	$C_{15}H_{10}O_6$	285.0394	3.80	5,7,2′,6′-Tetrahydroxyflavone	Polyhydroxylated flavone
17	17.696	$C_{15}H_{10}O_4$	253.0497	3.64	Chrysin	Flavone
18	17.700	$C_{21}H_{18}O_{10}$	429.0813	3.08	Chrysin 7-*O*-β-D-glucuronide	Flavone glycoside
19	17.829	$C_{15}H_{11}NO_4$	268.0611	1.8	Dielsiquinone	Alkaloids
20	18.772	$C_{15}H_{10}O_5$	269.0448	4.06	Apigenin	Flavone
21	19.701	$C_{15}H_{10}O_4$	253.0495	4.23	3,7-Dihydroxyflavone	Flavone
22	20.481	$C_{10}H_{13}NO_3$	194.0819	1.87	*n*-acetyldopamine	Phenolic amide

Note: RT = retention time.

4. Conclusions

This study suggests that the *O. indicum* extracts obtained via MAE, a green extraction technology, exhibit preliminary antioxidant, in vitro cytotoxic, and anti-inflammatory potential. All plant parts extracted using MAE with 50% (*v*/*v*) or 70% (*v*/*v*) ethanol showed antioxidant activity against DPPH radicals. Notably, most extracts prepared with 70% (*v*/*v*) ethanol demonstrated significant inhibition of nitric oxide (NO) production in RAW 264.7 macrophage cells. FTIR and LC-MS/MS analyses suggested the presence of phytochemical compounds, particularly flavonoids, flavonoid glycosides, methoxylated flavones, isoflavones, phenolic glycosides, and sugar-related metabolites, in selected extracts such as MAE-OL50, MAE-OB70, MAE-OL70, and MAE-OS70. These compounds are likely responsible for the observed antioxidant and anti-inflammatory effects. However, the phytochemicals were tentatively identified without authentic standards and were not quantified; their identities and contributions therefore require confirmation. These findings highlight the preliminary potential of *O. indicum* extracts as candidate active ingredients for cosmetic formulations targeting inflammation-associated and oxidative stress-

related skin concerns, such as acne-prone skin. Nevertheless, since this study is limited to preliminary antioxidant (DPPH) and anti-inflammatory (NO inhibition) screening assays, further studies including quantification of pro-inflammatory cytokines and analysis of relevant signaling pathways are needed to elucidate the underlying mechanism of action. Toxicological studies and further evaluation of efficacy involving human volunteers of cosmetic formulations based on these plant extracts are also required.

Supplementary Materials: The following supporting information can be downloaded at: https://www.mdpi.com/article/10.3390/cosmetics13060309/s1, Table S1: Tentative identification of phytochemical constituents in the 50% (*v*/*v*) ethanol extract of *Oroxylum indicum* leaf (MAE-OL50) performed via LC-QTOF-MS/MS in negative mode; Table S2: Tentative identification of phytochemical constituents in the 70% (*v*/*v*) ethanol extract of *Oroxylum indicum* leaf (MAE-OL70) performed via LC-QTOF-MS/MS in negative mode; Table S3: Tentative identification of phytochemical constituents in the 70% (*v*/*v*) ethanol extract of *Oroxylum indicum* bark (MAE-OB70) performed via LC-QTOF-MS/MS in negative mode; Table S4: Tentative identification of phytochemical constituents in the 70% (*v*/*v*) ethanol extract of *Oroxylum indicum* seed (MAE-OS70) performed via LC-QTOF-MS/MS.

Author Contributions: Conceptualization, T.T.; methodology, P.R., S.P., S.T., S.S. and P.C.; investigation, P.R., S.P., S.T., S.S. and P.C.; writing—original draft preparation, P.R. and T.T.; writing—review and editing, L.N., S.D.S. and T.T.; visualization, T.T.; supervision, T.T.; project administration, T.T.; funding acquisition, T.T. All authors have read and agreed to the published version of the manuscript.

Funding: This work was supported by Mae Fah Luang University, Thailand Science Research and Innovation (TSRI), and National Science, Research and Innovation Fund (NSRF) (Grant no. 682A02014), as well as the Graduate Research Grant, Mae Fah Luang University (Grant no. 19/66).

Institutional Review Board Statement: Not applicable.

Informed Consent Statement: Not applicable.

Data Availability Statement: The data used in this study are all available within this article. Further inquiries can be directed to the corresponding author.

Acknowledgments: We would like to thank the Scientific and Technological Instruments Centre, Mae Fah Luang University. We are grateful to Poramet Nachalaem for providing access to the mass spectrometric facilities. The authors acknowledge the use of the following generative AI tools for language editing: Claude (Anthropic; Claude Sonnet 5.5), ChatGPT (OpenAI, GPT-6.1), and Gemini (Google; Gemini 3).

Conflicts of Interest: The authors declare no conflicts of interest.

Abbreviations

DMSO	dimethyl sulfoxide
DPPH	2,2-diphenyl-1-picrylhydrazyl
FTIR	Fourier transform infrared spectroscopy
iNOS	inducible nitric oxide synthase
LC–MS/MS	liquid chromatography–tandem mass spectrometry
LPS	lipopolysaccharide
MAE	microwave-assisted extraction
NF-κB	nuclear factor kappa B
NO	nitric oxide
PCA	principal component analysis
ROS	reactive oxygen species
SD	standard deviation

UHPLC	ultra-high-performance liquid
UV–Vis	ultraviolet–visible spectroscopy
Q-TOF	quadrupole-time of flight

References

1. Vasam, M.; Korutla, S.; Bohara, R.A. Acne vulgaris: A review of the pathophysiology, treatment, and recent nanotechnology-based advances. *Biochem. Biophys. Rep.* **2023**, *36*, 101578. https://doi.org/10.1016/j.bbrep.2023.101578.
2. De Cruz, R.; Nguyen, R.; Chen, P.; Kerob, D.; Gebauer, K.; Willems, A.; Tong, P.; Lee, M. From Monotherapy to Adjunctive Therapies: Application of Dermocosmetics in Acne Management Across Australia and New Zealand. *Australas. J. Dermatol.* **2025**, *66*, 189–198. https://doi.org/10.1111/ajd.14447.
3. Zouboulis, C.C.; Coenye, T.; He, L.; Kabashima, K.; Kobayashi, T.; Niemann, C.; Nomura, T.; Oláh, A.; Picardo, M.; Quist, S.R.; et al. Sebaceous immunobiology—Skin homeostasis, pathophysiology, coordination of innate immunity and inflammatory response and disease associations. *Front. Immunol.* **2022**, *13*, 1029818. https://doi.org/10.3389/fimmu.2022.1029818.
4. Eichenfield, D.Z.; Sprague, J.; Eichenfield, L.F. Management of acne vulgaris: A review. *JAMA* **2021**, *326*, 2055. https://doi.org/10.1001/jama.2021.17633.
5. Cruz, S.; Vecerek, N.; Elbuluk, N. Targeting Inflammation in Acne: Current Treatments and Future Prospects. *Am. J. Clin. Dermatol.* **2023**, *24*, 681–694. https://doi.org/10.1007/s40257-023-00789-1.
6. Mias, C.; Mengeaud, V.; Bessou-Touya, S.; Duplan, H. Recent advances in understanding inflammatory acne: Deciphering the relationship between *Cutibacterium acnes* and Th17 inflammatory pathway. *J. Eur. Acad. Dermatol. Venereol.* **2023**, *37*, 3–11. https://doi.org/10.1111/jdv.18794.
7. Huang, T.Y.; Jiang, Y.E.; Scott, D.A. Culturable bacteria in the entire acne lesion and short-chain fatty acid metabolites of *Cutibacterium acnes* and *Staphylococcus epidermidis* isolates. *Biochem Biophys. Res. Commun.* **2022**, *622*, 45–49. https://doi.org/10.1016/j.bbrc.2022.06.068.
8. Podwojniak, A.; Tan, I.J.; Sauer, J.; Neubauer, Z.; Rothenberg, H.; Ghani, H.; Parikh, A.K.; Cohen, B. Acne and the cutaneous microbiome: A systematic review of mechanisms and implications for treatments. *J. Eur. Acad. Dermatol. Venereol.* **2025**, *39*, 793–805. https://doi.org/10.1111/jdv.20332.
9. Joompang, A.; Phosri, S.; Wisetsai, A. Chemical constituents and their anti-inflammatory activity of *Ochna integerrima* roots. *Nat. Prod. Res.* **2025**, *40*, 4696–4702. https://doi.org/10.1080/14786419.2025.2480662.
10. Zhao, D.; Wang, Y.; Wu, S.; Ji, X.; Gong, K.; Zheng, H.; Zhu, M. Research progress on the role of macrophages in acne and regulation by natural plant products. *Front. Immunol.* **2024**, *15*, 1383263. https://doi.org/10.3389/fimmu.2024.1383263.
11. Popa, G.L.; Mitran, C.I.; Mitran, M.I.; Tampa, M.; Matei, C.; Popa, M.I.; Georgescu, S.R. Markers of oxidative stress in patients with acne: A literature review. *Life* **2023**, *13*, 1433. https://doi.org/10.3390/life13071433.
12. Morris, G.; Gevezova, M.; Sarafian, V.; Maes, M. Redox regulation of the immune response. *Cell Mol. Immunol.* **2022**, *19*, 1079–1101. https://doi.org/10.1038/s41423-022-00902-0.
13. Rizo-Téllez, S.A.; Filep, J.G. Beyond host defense and tissue injury: The emerging role of neutrophils in tissue repair. *Am. J. Physiol. Cell Physiol.* **2024**, *326*, C661–C683. https://doi.org/10.1152/ajpcell.00652.2023.
14. Panomai, P.; Thapphasaraphong, S.; Nualkaew, N. A Comparative Study of Two *Oroxylum indicum* (L.) Kurz. Phenotypes Based on Phytochemicals and Antioxidant Effects, and the Anti-Inflammatory Activity of Leaf and Pod Extracts. *Plants* **2024**, *13*, 2110. https://doi.org/10.3390/plants13152110.
15. Rojsanga, P.; Schwaiger, S.; Stuppner, H.; Sithisarn, P. Determination of Phytochemical Contents in Extracts from Different Growth Stages of *Oroxylum indicum* Fruits Using HPLC-DAD and QAMS Methods. *Molecules* **2023**, *28*, 6837. https://doi.org/10.3390/molecules28196837.
16. Srimawong, C.; Putalun, W. Consolidated extraction and conversion of baicalin to baicalein from *Oroxylum indicum* using a novel NADES-UAE system and bioactivity evaluation in RAW 264.7 cells. *Food Biosci.* **2025**, *65*, 106031. https://doi.org/10.1016/j.fbio.2025.106031.
17. Choonong, R.; Waewaram, V.; Buraphaka, H.; Krittanai, S.; Boonsnongcheep, P.; Putalun, W. Anti-inflammatory potential of *Oroxylum indicum* flavonoids: Effects of traditional grilling on aglycone flavonoid content and activity against urban dust-induced inflammation. *Food Biosci.* **2024**, *62*, 105523. https://doi.org/10.1016/j.fbio.2024.105523.
18. Rodwattanagul, S.; Wongrattanakamon, P.; Chaichit, S.; Chittasupho, C.; Nimlamool, W.; Hennink, W.E.; Okonogi, S. Exploring the antioxidant, antiglycation, and anti-inflammatory potential of *Oroxylum indicum* stem bark extracts. *PLoS ONE* **2025**, *20*, e0325795. https://doi.org/10.1371/journal.pone.0325795.

19. Nguyen, H.L.; Sae-Eaw, A.; Tran, D.Q.; Prinyawiwatkul, W.; Chulikhit, Y. A Systematic Review of Evidence-Based Health Benefits of *Oroxylum indicum* and Its Functional Food Potential. *Foods* **2025**, *14*, 3465. https://doi.org/10.3390/foods14203465.
20. Rai, D.; Aswatha Ram, H.N.; Neeraj Patel, K.; Babu, U.V.; Sharath Kumar, L.M.; Kannan, R. In vitro immuno-stimulatory and anticancer activities of *Oroxylum indicum* (L.) Kurz.: An evidence for substitution of aerial parts for conservation. *J. Ayurveda Integr. Med.* **2022**, *13*, 100523. https://doi.org/10.1016/j.jaim.2021.09.001.
21. Sithisarn, P.; Rojsanga, P.; Sithisarn, P. Flavone-rich fractions and extracts from *Oroxylum indicum* and their antibacterial activities against clinically isolated zoonotic bacteria and free radical scavenging effects. *Molecules* **2021**, *26*, 1773. https://doi.org/10.3390/molecules26061773.
22. Yan, K.; Cheng, X.; Bian, G.; Gao, Y.; Li, D. The influence of different extraction techniques on the chemical profile and biological properties of *Oroxylum indicum*: Multifunctional aspects for potential pharmaceutical applications. *Evid.-Based Complement. Altern. Med.* **2022**, *2022*, 8975320. https://doi.org/10.1155/2022/8975320.
23. Ferrara, D.; Beccaria, M.; Cordero, C.E.; Purcaro, G. Microwave-assisted extraction in closed vessel in food analysis. *J. Sep. Sci.* **2023**, *46*, e2300390. https://doi.org/10.1002/jssc.202300390.
24. Gunalan, S.; Thangaiah, A.; Rathnasamy, V.K.; Janaki, J.G.; Thiyagarajan, A.; Kuppusamy, S.; Arunachalam, L. Microwave-assisted extraction of biomolecules from Moringa (*Moringa oleifera* Lam.) leaves Var. PKM 1: A optimization study by response surface methodology (RSM). *Kuwait J. Sci.* **2023**, *50*, 339–344. https://doi.org/10.1016/j.kjs.2023.01.001.
25. de Oliveira, F.M.G.; Lyrio, M.V.V.; Filgueiras, P.R.; de Castro, E.V.R.; Kuster, R.M. ESI(-)FT-ICR MS for the determination of best conditions for producing extract abundant in phenolic compounds from leaves of *E. uniflora* and FTIR-PCA as a sample screening method. *Anal. Methods* **2024**, *16*, 3701–3713. https://doi.org/10.1039/d3ay00773a.
26. Peng, Y.; Bie, S.; Cai, S.; Zhou, L.; Guo, C. Effects of high-pressure homogenization on phenolics profile, antioxidant activity, α-glucosidase inhibitory activity, and insulin resistance of peach juice during simulated gastrointestinal digestion. *Food Chem. X* **2025**, *26*, 102263. https://doi.org/10.1016/j.fochx.2025.102263.
27. Na Nongkhai, T.; Maddocks, S.E.; Phosri, S.; Sangthong, S.; Pintathong, P.; Chaiwut, P.; Chandarajoti, K.; Nahar, L.; Sarker, S.D.; Theansungnoen, T. In Vitro Cytotoxicity and Antimicrobial Activity against Acne-Causing Bacteria and Phytochemical Analysis of Galangal (*Alpinia galanga*) and Bitter Ginger (*Zingiber zerumbet*) Extracts. *Int. J. Mol. Sci.* **2024**, *25*, 10869. https://doi.org/10.3390/ijms252010869.
28. Yubolphan, R.; Phongsiri, K.; Mongkhammee, N.; Pidech, J.; Roytrakul, S.; Suwattanasophon, C.; Choowongkomon, K.; Daduang, S.; Khunkitti, W.; Jangpromma, N. Anti-Inflammatory Effects of Hen Egg White Hydrolysate and Its Specific Peptides IS8, PA11, and PK8 on LPS-Induced Macrophage Inflammation. *Food Sci. Nutr.* **2025**, *13*, e70713. https://doi.org/10.1002/fsn3.70713.
29. Phosri, S.; Kiattisin, K.; Intharuksa, A.; Janon, R.; Na Nongkhai, T.; Theansungnoen, T. Anti-aging, anti-acne, and cytotoxic activities of *Houttuynia cordata* extracts and phytochemicals analysis by LC-MS/MS. *Cosmetics* **2022**, *9*, 136. https://doi.org/10.3390/cosmetics9060136.
30. Buachoon, N. Optimization of solvent systems and extraction techniques for enhanced multifunctional bioactivities of *Vernonia cinerea* (L.) Less.: A comprehensive study on antioxidant, tyrosinase inhibitory, antibacterial, and antidiabetic enzyme activities. *TiS* **2025**, *22*, 11007. https://doi.org/10.48048/tis.2026.11007.
31. Begum, M.M.; Islam, A.; Begum, R.; Uddin, M.S.; Rahman, M.S.; Alam, S.; Akter, W.; Das, M.; Rahman, M.S.; Imon, A.H.M.R. Ethnopharmacological inspections of organic extract of *Oroxylum indicum* in rat models: A promising natural gift. *Evid.-Based Complement. Altern. Med.* **2019**, *2019*, 1562038. https://doi.org/10.1155/2019/1562038.
32. Cobzac, S.C.A.; Casoni, D.; Badea, M.; Balabanova, B.; Markova Ruzdik, N. Ultraviolet-visible (UV-Vis) spectroscopy and cluster analysis as a rapid tool for classification of medicinal plants. *Stud. UBB Chem.* **2019**, *64*, 191–203. https://doi.org/10.24193/subbchem.2019.4.14.
33. Casoni, D.; Cobzac, S.C.A.; Simion, I.M. Feasibility of UV–Vis Spectroscopy combined with pattern recognition techniques to authenticate the medicinal plant material from different geographical areas. *J. Anal. Sci. Technol.* **2024**, *15*, 17. https://doi.org/10.1186/s40543-024-00428-2.
34. Faraz, R.; Gokhale, M.; Gothalwal, R. Callus extracts of *Oroxylum indicum* (L.) Vent containing baicalein have in vitro antioxidant and antibacterial activities. *Biotecnol. Veg.* **2020**, *20*, 51–62.
35. Sutariya, S.; Ahmad Shah, A.; Bajpai, A.B.; Sharma, R.J.; Pandhurnekar, C.P.; Gupta, A. Fourier transform infrared spectroscopy (FTIR) analysis, antioxidant and anti-inflammatory activities of leaf and fruit extracts of *Gymnosporia montana*. *Mater. Today Proc.* **2023**, *73*, 134–141. https://doi.org/10.1016/j.matpr.2022.09.462.

36. Boutagayout, A.; Lahlali, R.; El Baghazaoui, R.; Bouiamrine, E.H.; Radah, A.; Benabderrahmane, A.; Adiba, A.; Hamdani, A.; El Oihabi, K.; Belmalha, S. GC–MS and FTIR analysis and effects of thyme (*Thymbra capitata* L. Cav) and rosemary (*Rosmarinus officinalis* L.) essential oils on the growth and pathogenicity of *Botrytis fabae*. *Int. J. Environ. Stud.* **2025**, *82*, 501–522. https://doi.org/10.1080/00207233.2024.2405448.
37. Noh, C.H.C.; Azmin, N.F.M.; Amid, A. Principal component analysis application on flavonoids characterization. *Adv. Sci. Technol. Eng. Syst. J.* **2017**, *2*, 435–440. https://doi.org/10.25046/aj020356.
38. Nikolova, K.; Eftimov, T.; Panova, N.; Vladev, V.; Fouzar, S.; Nikolov, K. Characterization of Bulgarian Rosehip Oil by GC-MS, UV-VIS Spectroscopy, Colorimetry, FTIR Spectroscopy, and 3D Excitation–Emission Fluorescence Spectra. *Molecules* **2025**, *30*, 3964. https://doi.org/10.3390/molecules30193964.
39. Vittaya, L.; Chalad, C.; Ratsameepakai, W.; Leesakul, N. Phytochemical characterization of bioactive compounds extracted with different solvents from *Calophyllum inophyllum* flowers and activity against pathogenic bacteria. *S. Afr. J. Bot.* **2023**, *154*, 346–355. https://doi.org/10.1016/j.sajb.2023.01.052.
40. Aouant, K.; Christodoulou, P.; Tsiaka, T.; Strati, I.F.; Cavouras, D.; Sinanoglou, V.J. Implementation of Instrumental Analytical Methods, Image Analysis and Chemometrics for the Comparative Evaluation of Citrus Fruit Peels. *Foods* **2025**, *14*, 4115. https://doi.org/10.3390/foods14234115.
41. Durak, T.; Depciuch, J. Effect of plant sample preparation and measuring methods on ATR-FTIR spectra results. *Environ. Exp. Bot.* **2020**, *169*, 103915. https://doi.org/10.1016/j.envexpbot.2019.103915.
42. Giorgini, E.; Notarstefano, V.; Foligni, R.; Carloni, P.; Damiani, E. First ATR-FTIR Characterization of Black, Green and White Teas (*Camellia sinensis*) from European Tea Gardens: A PCA Analysis to Differentiate Leaves from the In-Cup Infusion. *Foods* **2024**, *13*, 109. https://doi.org/10.3390/foods13010109.
43. Nigam, M.; Gandhi, Y.; Kumar, V.; Soni, H.; Saxena, R.K. Quantification of phytochemicals of different parts of *Oroxylum indicum* (L.) Kurz for the evidence-based substitution of the official part (root) with aerial part. *Talanta Open* **2025**, *12*, 100528. https://doi.org/10.1016/j.talo.2025.100528.
44. Sithisarn, P.; Nantateerapong, P.; Rojsanga, P.; Sithisarn, P. Screening for antibacterial and antioxidant activities and phytochemical analysis of *Oroxylum indicum* fruit extracts. *Molecules* **2016**, *21*, 446. https://doi.org/10.3390/molecules21040446.
45. Abdulhafiz, F.; Reduan, M.F.H.; Hisam, A.H.; Mohammad, I.; Abdul Wahab, I.R.; Abdul Hamid, F.F.; Mohammed, A.; Nordin, M.L.; Shaari, R.; Bakar, L.A.; et al. LC–TOF–MS/MS and GC-MS based phytochemical profiling and evaluation of wound healing activity of *Oroxylum indicum* (L.) Kurz (Beka). *Front. Pharmacol.* **2022**, *13*, 1050453. https://doi.org/10.3389/fphar.2022.1050453.
46. Kameyanda Poonacha, S.; Harishkumar, M.; Radha, M.; Varadarajan, R.; Nalilu, S.K.; Shetty, S.S.; Shetty, P.K.; Chandrashekharappa, R.B.; Sreenivas, M.G.; Bhandary Bavabeedu, S.K. Insight into oroxylinA–7–O–β–d-glucuronide-enriched *Oroxylum indicum* bark extract in oral cancer HSC–3 cell apoptotic mechanism: Role of mitochondrial microenvironment. *Molecules* **2021**, *26*, 7430. https://doi.org/10.3390/molecules26247430.
47. Dunkhunthod, B.; Talabnin, C.; Murphy, M.; Thumanu, K.; Sittisart, P.; Hengpratom, T.; Eumkeb, G. Intracellular ROS scavenging and anti-inflammatory activities of *Oroxylum indicum* Kurz (L.) extract in LPS plus IFN- γ -activated RAW264.7 macrophages. *Evid.-Based Complement. Altern. Med.* **2020**, *2020*, 7436920. https://doi.org/10.1155/2020/7436920.
48. Intharuksa, A.; Arunotayanun, W.; Na Takuathung, M.; Chaichit, S.; Prasansuklab, A.; Chaikhong, K.; Sirichanchuen, B.; Chupradit, S.; Koonrungsesomboon, N. Daidzein and Genistein: Natural Phytoestrogens with Potential Applications in Hormone Replacement Therapy. *Int. J. Mol. Sci.* **2025**, *26*, 6973. https://doi.org/10.3390/ijms26146973.
49. Ren, F.; Li, Y.; Luo, H.; Gao, S.; Jiang, S.; Yang, J.; Rao, C.; Chen, Y.; Peng, C. Extraction, detection, bioactivity, and product development of luteolin: A review. *Heliyon* **2024**, *10*, e41068. https://doi.org/10.1016/j.heliyon.2024.e41068.
50. Navarro-Hoyos, M.; Bisoyi, R.; Kc, P.; Lutz, N.; Ruxsarash, M. Key Dietary Flavonoids: Insights into Their Structural Characteristics, Antioxidant and Anti-Inflammatory Activities, and Potential as Neuroprotective Agents. *Molecules* **2026**, *31*, 154. https://doi.org/10.3390/molecules31010154.
51. Hu, Z.; Guan, Y.; Hu, W.; Xu, Z.; Ishfaq, M. An overview of pharmacological activities of baicalin and its aglycone baicalein: New insights into molecular mechanisms and signaling pathways. *Iran. J. Basic Med. Sci.* **2022**, *25*, 14–26. https://doi.org/10.22038/IJBMS.2022.60380.13381.
52. Aghababaei, F.; Hadidi, M. Recent advances in potential health benefits of quercetin. *Pharmaceuticals* **2023**, *16*, 1020. https://doi.org/10.3390/ph16071020.
53. Han, L.; Yuan, Y.; Chen, X.; Huang, J.; Wang, G.; Zhou, C.; Dong, J.; Zhang, N.; Zhang, Y.; Yin, H.; et al. A Candidate Drug Screen Strategy: The Discovery of Oroxylin A in Scutellariae Radix Against Sepsis via the Correlation Analysis Between Plant Metabolomics and Pharmacodynamics. *Front Pharmacol.* **2022**, *13*, 861105. https://doi.org/10.3389/fphar.2022.861105.

Disclaimer/Publisher's Note: The statements, opinions and data contained in all publications are solely those of the individual author(s) and contributor(s) and not of MDPI and/or the editor(s). MDPI and/or the editor(s) disclaim responsibility for any injury to people or property resulting from any ideas, methods, instructions or products referred to in the content.

https://doi.org/10.3390/cosmetics13060309